Mathematical Biosciences and Engineering

MBE, 20(5): 9572–9606.
DOI: 10.3934/mbe.2023420
Received: 25 November 2022
Revised: 21 January 2023
Accepted: 01 February 2023
Published: 21 March 2023

http://www.aimspress.com/journal/MBE

Research article

Computational systems biology approach for permanent tumor elimination and normal tissue protection using negative biasing: Experimental validation in malignant melanoma as case study

Bindu Kumari[1], Chandrashekhar Sakode[2], Raghavendran Lakshminarayanan[3] and Prasun K. Roy[1,4,*]

[1] School of Biomedical Engineering, Indian Institute of Technology (BHU), Varanasi 221005, India
[2] Department of Applied Sciences, Indian Institute of Information Technology, Nagpur 44005, India
[3] School of Computational Sciences, Jawaharlal Nehru University, New Delhi 110067, India
[4] Department of Life Sciences, Shiv Nadar University (SNU), Delhi NCR, Dadri 201314, India

* **Correspondence:** Email: prasun.roy@snu.edu.in; Tel: +919910831172.

Abstract: Complete spontaneous tumor regression (without treatment) is well documented to occur in animals and humans as epidemiological analysis show, whereby the malignancy is permanently eliminated. We have developed a novel computational systems biology model for this unique phenomenon to furnish insight into the possibility of therapeutically replicating such regression processes on tumors clinically, without toxic side effects. We have formulated oncological informatics approach using cell-kinetics coupled differential equations while protecting normal tissue. We investigated three main tumor-lysis components: (i) DNA blockade factors, (ii) Interleukin-2 (IL-2), and (iii) Cytotoxic T-cells ($CD8^+$ T). We studied the temporal variations of these factors, utilizing preclinical experimental investigations on malignant tumors, using mammalian melanoma microarray and histiocytoma immunochemical assessment. We found that permanent tumor regression can occur by: 1) Negative-Bias shift in population trajectory of tumor cells, eradicating them under first-order asymptotic kinetics, and 2) Temporal alteration in the three antitumor components (DNA replication-blockade, Antitumor T-lymphocyte, IL-2), which are respectively characterized by the following patterns: (a) Unimodal Inverted-U function, (b) Bimodal M-function, (c) Stationary-step function. These provide a time-wise orchestrated tri-phasic cytotoxic profile. We have also elucidated gene-expression levels corresponding to the above three components: (i) DNA-damage G2/M checkpoint

regulation [genes: *CDC2-CHEK*], (ii) Chemokine signaling: IL-2/15 [genes: *IL2RG-IKT3*], (iii) T-lymphocyte signaling (genes: *TRGV5-CD28*). All three components quantitatively followed the same activation profiles predicted by our computational model (Smirnov-Kolmogorov statistical test satisfied, α = 5%). We have shown that the genes *CASP7-GZMB* are signatures of Negative-bias dynamics, enabling eradication of the residual tumor. Using the negative-biasing principle, we have furnished the dose-time profile of equivalent therapeutic agents (DNA-alkylator, IL-2, T-cell input) so that melanoma tumor may therapeutically undergo permanent extinction by replicating the spontaneous tumor regression dynamics.

Keywords: negative bias; systems biology; spontaneous cancer regression; chemotherapy; bioinformatics; immunotherapy; melanoma; histiocytoma; microarray

1. Introduction

There are several significant drawbacks to cancer treatment by antitumor agents, as chemotherapy and immunotherapy. The first issue is an apparent "clinical cure" whereby the tumor cells are eliminated to a major extent, so that the tumor is clinically undetectable, even though microscopic amounts of cancer cells remain, which flare up much later after the initial therapy, thus producing tumor recurrence. The second is presence of cancer stem cells which, even though initially forming an miniscule cellular population, goes on multiplying as they have much less sensitivity to therapeutic agents, thus producing resistant tumor relapse [1]. Another issue is the inability of administering therapeutic agents intensively, as the latter produces appreciable normal tissue damage, producing intolerable side-effects that prevent the administration of further therapy. These disadvantages need to be well addressed, even though it is also known that occasionally there is permanent elimination of a tumor by exogenous therapeutic agents. Some examples of such exogenous regression of tumors are multimodal chemoimmunotherapy using drugs (like alkylators as dacarbazine or temozolomide), antitumor lymphocyte therapy, along with interleukin [2,3].

Though the clinician usually encounters a malignant tumor in its progression phase, the reverse process of permanent spontaneous regression of malignant tumors is a well-documented phenomenon, occurring subclinically across human populations at 22–46% rate, as per the Scandinavian and Wisconsin Screening Registries which have tracked a population of 0.33 million and 2.95 million individuals respectively [4,5]. It is evident in autopsy studies that about half the subjects have malignant focus in uterine cervix or prostate, with confirmation of permanent containment, and furthermore, malignant neuroblastoma fully regresses from larger-sized tumors [4,6]. As per PubMed, there are about 14,000 titles of papers dealing with spontaneous cancer regression, covering virtually all types of malignant diseases such as sarcomas, carcinomas, lymphomas, melanomas and so on [7]. Though the regression process eliminates malignant cells, it does not damage the normal tissue, i.e. normal cells are protected overall. Typically, the duration of a tumor's regression generally occurs across a period of months, generally 1 to 2 months. Such endogenously-initiated regression of malignancy also occurs in animals, including worms and molluscs and even took place in dinosaurs which are now extinct [8]. In fact, there are numerous species of animals known to completely regress malignant lesions, which are usually fatal in man, such as melanoma. We have earlier elucidated the

energetics and biothermodynamic basis of spontaneous tumor regression [9,10]. Indeed, the investigation of the spontaneous regression process may indicate incisive pointers on inducing the permanent regression process on human malignancies.

Spontaneous cancer regression (both endogenous or exogenous process) depends on various factors like the amount of the tumor load, the invasiveness of the disease, the intensity of the treatment, and the robustness of the patient's immune response. Mathematical modeling is seen to be a potentially vital tool for creating better treatment strategies for cancer patients to address the cancer regression process. Over the years, researchers have used various models to address the biological process of tumor growth and of anticancer treatment [11–14]. In this study we have considerably modified our previously developed model [15], in which tumor cell kinetics, chemotherapy dynamics, dynamics of immune system (NK cell, circulating lymphocyte and cytotoxic T-cell), chemotherapy dynamics, and immunomodulation/immunotherapy dynamics, are represented by a system of six differential equations. Our novel mathematical model is incisively based on experimentally observed biological processes, namely the lethal effect on the tumor cell, as induced by the immune cells, namely cytotoxic T-cells ($CD8^+$), and natural killer (NK) cells, the delineation of these lethal interactions are delineated next.

It is well established that NK cells target tumor cells and produce cytokines by secreting perforins and granzymes as part of immune responses to malignancies [16,17]. These immune cells release perforins in the immunological synapse, the perforins are pore-forming cytolytic protein that form porous openings in the tumor cell membrane [18]. Once this occurs, the immune cells release granzyme, which is a proteolytic enzyme that travels through the pore into the cytoplasm of the tumor cell, activating the caspase cascade and thereby inducing programmed cell death or apoptosis in the malignant cell [19]. When NK cells and T-cells come into contact with cancer cells, immunological synapses are formed with tumor cells to deliver lysosome-mediated cytolytic agents (as cathepsins and hydrolases) inside the tumor cells [20]. Moreover, granzymes and perforin are two further examples of cytotoxic chemicals that $CD8^+$ T cells can use to kill tumor cells. Additionally, chemokines as interferons (which cytotoxic $CD8^+$ T-cells secrete) can activate the tumor cells to produce more MHC class I antigens, making the malignant cells to become more attractive targets for cytotoxic $CD8^+$ T-cells [21].

In this paper, we attempt to quantitatively formulate the general methodology of complete tumor regression (whether endogenous or exogenous) and discern the unitary principles that enable this regression. Thereafter, the validation of the methodology in pre-clinical environment are shown on two malignant systems, melanoma and histiocytoma. To underscore, melanoma cases can undergo fully effective spontaneous regression (PubMed has 585 cases studied in detail [22]), and this melanoma regression occurs appreciably at 10–35% rate [23]. Analysis of 10,098 melanoma regression patients showed that these patients can have incisive clinical correlates [24]. Understanding melanoma regression is critically needed, as it is the type of malignancy whose incidence is accelerating maximally [25]. An important aspect here is that we have showed that a malignant lesion can undergo permanent regression by an optimized synchronization of: 1) antitumor feedback control process, based on optimal dynamic feedback according to tumor load, and 2) normal tissue protection, based on minimization of tissue toxicity, together with 3) ensuring that cancer stem cells are also eliminated. In contrast to this permanent regression approach, we also show that often conventionally dosed antitumor chemotherapy-immunotherapy intervention (i.e., without dynamic feedback control procedure) fails to eliminate the tumor cells completely, with the result that there is tumor recurrence later.

Various differential equation-based quantitative models are available in the literature to replicate the dynamics of the biological process of cancer regression, and some of these models will be delineated now. For instance, Perry [9] has used the laws of mass action and first-order dynamics to characterize the reaction kinetics of tumor cell lysis during exogenous tumor regression brought on by therapeutic agents such as chemotherapy medications that cause DNA damage in the malignant lesion. As a result, the tumor cell population T declines exponentially [9]. Furthermore, when a lesion spontaneously regresses, the tumor cell population reduces exponentially with time [26,27]. However, a residual tumor cell population asymptotically exists under the exponentially-decreasing trajectory and this population of residual cells is frequently a factor in tumor recurrence and incurability. It is well-known that three complementary processes can reduce the tumor cell population:

(i) Decrease of the proliferation of tumor cells: Here, chemical alkylation or chemomodulation of DNA are two methods for reducing cell proliferation that can lead to DNA damage [28,29],
(ii) Increase of tumor cell lysis: This occurs through the medium of antitumor lymphocytes [18,30,31],
(iii) Further enhancement of tumor cell lysis: The activation of the antitumor lymphocytes can be boosted by cytokines (for example, immunomodulation by interleukin-2) [32].

The mathematical framework of these three processes have been developed by de Pillis et al. [33], Kuznetsov et al. [34] , and Kirschner et al. [35] based on experimental data, and the predictions of the modelling have also been empirically validated [36]. These models effectively describe the computational dynamics of antitumor activity by DNA damage and immunological action. However, in all these models, the tumor cell population follows first-order biochemical kinetics and exponential asymptotic decay of tumor population with some residual malignant cells remaining, and complete eradication of all tumor cell fails to occur, and thus future relapse of the cancer lesion happens. In this study we aim to improve the aforesaid models using our procedure. The methodology of this paper can remove the aforesaid asymptotic cancer cell population, and enable eradication of all malignant cells, with permanent elimination of the tumor without any future recurrence.

It may be underscored that our analysis of the extinction of cancer cells is motivated from the well-known process of spontaneous permanent regression of tumors and its system biology evidence, whereby we have developed an approach of how one can replicate this tumor regression process in a clinical situation. We have provided substantiation of the proposed feedback approach by quantitative analysis of signal transduction pathway, gene expression level of G2/M-phase DNA damage pathway, IL-2 expression and T-cell receptor signaling. Finally, the translational aspects and validated corroboration of our approach is furnished, which enables the formulation of a guided controller-based treatment planning system governing the infusion of chemotherapy, interleukin, and antitumor T-cell immunotherapy, for complete extinction of the malignant lesion, cancer stem cell elimination and normal tissue protection. For a comprehensive understanding, Schema 1 summarizes our problem statement and our approach to it.

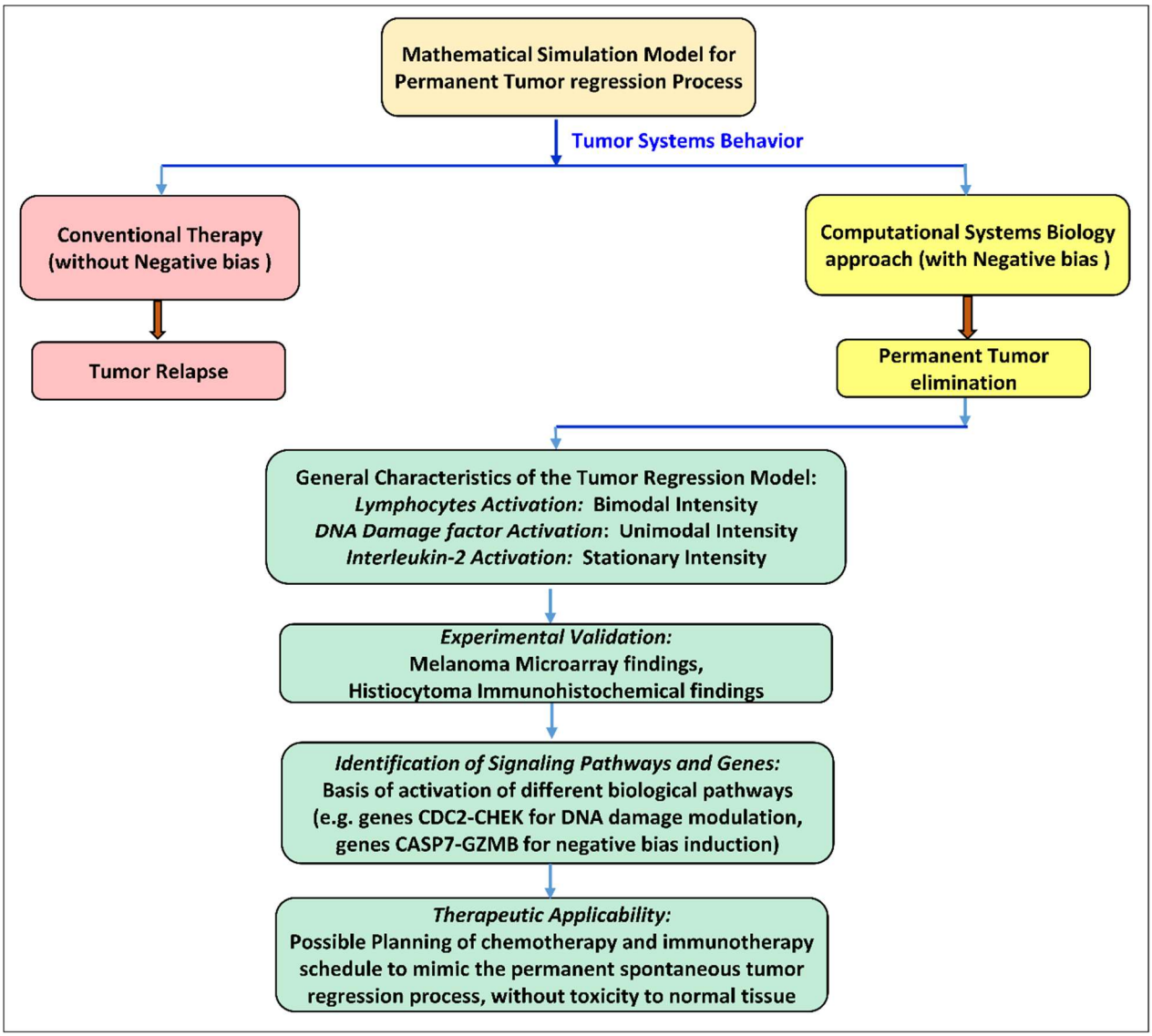

Schema 1. Workflow of the problem statement and our approach to elucidate it.

2. Materials and methods:

2.1. Formulating the computational framework of spontaneous tumor regression:

During exogenous tumor regression induced by therapeutic agents such as chemotherapy drugs that induce DNA damage, the reaction kinetics of tumor cell lysis is described by laws of mass action and first-order dynamics, hence the tumor cell population M decreases exponentially [9]. Likewise, in endogenous or spontaneous regression of tissue lesion or malignancy, the tumor cell population exponentially decreases with time [26,27,37]. For instance, in the former experiment [9], the proliferative cell activity is estimated by metabolic phosphorylation intensity, namely by ATP dynamics. Thus, the trajectory is $M = M_0 exp(-\varepsilon t)$, where ε, the rate parameter, is the intensity of the tumor regression effect (Figure 1(a)). Typically, a clinically just-detectable tumor has 10^7 malignant cells, and for regression in a reasonable time (say 1–2 months), this tumor cell population can decrease

essentially to near zero (say 0.01 of cell population, or 10^{-4} of cell population), which can be enabled by using a suitable value of the rate parameter, induced by the regression process.

It may be noted here that there always persists asymptotically a residual tumor cell population under the trajectory and this can often be the factor of tumor recurrence. However, one can resolve the asymptotic issue and enable the tumor population trajectory to become zero at a definitive time point, using the principle of negative biasing by following a path of guided control [38,39]. Here the tumor cell trajectory exponentially approaches a negative value M*, indicating that the tumor cell population trajectory becomes zero at time t_F (Figure 1(b)). This indicates that $M = [(M_0+M^*)exp(-\varepsilon t)]- M^*$, so that bias $M^*= -M_0\exp(-\varepsilon t_F)/(1-\exp(-\varepsilon t_F))$.

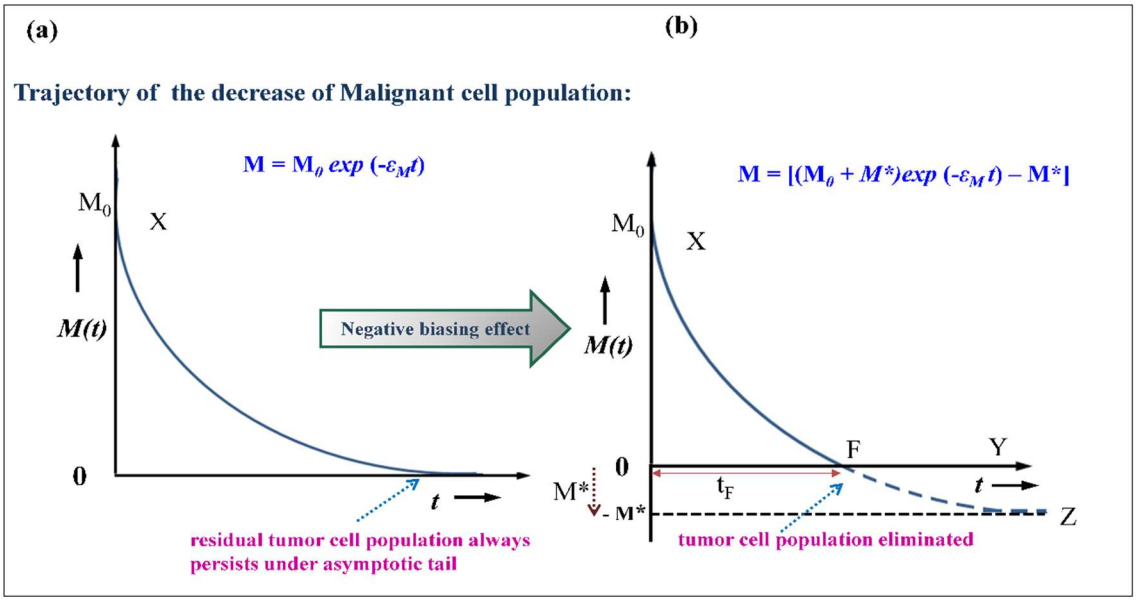

Figure 1. Complete tumor elimination process by principle of negative biasing. (a): In conventional therapy, the elimination of the tumor cell population M(t) follows an exponentially-decreasing trajectory, with tumor cells always persisting asymptotically under the curve, thereby leading to tumor relapse after therapy duration has ended. (b): The Negative bias shift process enables the residual tumor cell population to become zero at a finite time t_F. This curve M(t) decreases exponentially by approaching the negative bias (–M*) value, so that, at time point F, it hits the horizontal *x*-axis, where tumor cell population is zero. Thus, at F the tumor cell population becomes extinct and there is no further tumor cell to replicate, i.e., complete and permanent tumor regression occurs, eliminating the malignant lesion.

2.2. Systems analysis of tumor extinction:

Regarding exogenous regression (therapy-initiated regression) and endogenous regression (tissue-initiated regression), we have formulated a multimodal equivalence of the two regression processes from a systems biology perspective. Thereby, as Figure 2 elucidates, the three input terms to the tumor-host system (boxes on left side), respectively correspond to the entities of DNA damage or cell-proliferation blockage, tumor-infiltrating lymphocytes, and cytokine as interleukin. For a

malignant tumor to undergo elimination, three complimentary processes for tumor cell reduction may need to occur:

(i) Decreasing the tumor cell proliferation: Proliferation of cells can be reduced by processes that enable DNA impairment, as by chemical alkylation or chemomodulation of DNA,

(ii) Increasing tumor cell lysis, for example, by antitumor lymphocyte formation,

(iii) Activation of these lymphocytes which can be enhanced by cytokines (for instance, immunomodulation by chemokines as interleukin-2).

Implementation of the aforesaid tumor regression processes can happen in two ways:

(a) Exogenous process, where the above three factors, DNA chemomodulation, antitumor lymphocyte formation and cytokine immunomodulation can be respectively induced by externally injecting alkylating chemotherapy drug, tumor infiltrating lymphocyte, and interleukin-2.

(b) Endogenous process, where the three factors are autogenously generated by the host tissue itself, such as, by DNA blockage, cytotoxic lymphocyte infiltration into the tumor, and interleukin-2 upregulation, respectively.

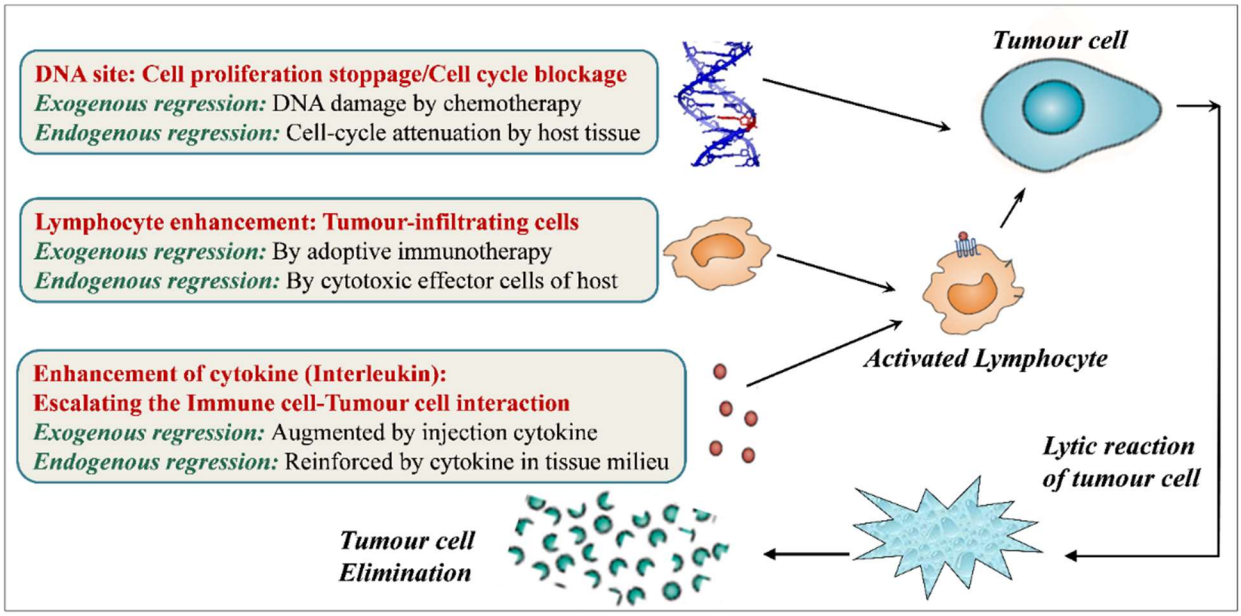

Figure 2. Multimodal equivalence between 1) Therapy-induced elimination of tumor, i.e., Exogenous tumor regression, and 2) Host tissue-induced elimination to tumor, i.e., Endogenous tumor regression. Endogenous regression of tumor is due to internally-generated factors, while Exogenous regression is due to externally-generated factors. Each of the three causative entities of Exogenous regression (therapy-initiated regression) and Endogenous regression (tissue-initiated regression) have similar factors, as detailed in the three boxed entities on the left side.

It should be mentioned here that the main route of DNA damage in both exogenous and endogenous tumor regression is by alkylation. For instance, in exogenous regression (e.g., by drugs), the DNA chemotherapy agents such as the most widely used pharmaceuticals as alkylators, function by alkylating the guanine moiety of DNA. Likewise, in endogenous regression (e.g., by spontaneous cancer regression), T-cell upregulation is a major factor, these cells secrete granzyme factor which

activates Trex enzyme that induces DNA single-strand breaks at the 3'-portion [18]. It is known that such single-strand breaks at 3'-portion function onwards by alkylating the adjacent guanine moiety of DNA [9]. We have worked out the quantitative equivalence between the dynamics of spontaneous tumor regression and of therapy-induced tumor regression in Section 1 of the Supplement.

We now endeavor to develop a quantitative analysis of endogenous or exogenous tumor regression. Consider the milieu of the tumor's interaction, namely the populations of malignant tumor cells, natural killer cells, and circulating white blood cells (lymphocytes in the blood), which can be denoted respectively by M, K, B (Figure 3). Let C, A and D denote the intensity levels respectively of IL-2 (e.g., concentration), of Antitumor lymphocyte (e.g., T-lymphotyte infiltration population), and of DNA chemomodulation, namely, DNA interference in cells, e.g., concentration level of DNA-damaging moieties in tumor tissue (Figure 3), which can be gauged by the level of TNFα or by the level of DNA damage's checkpoint activation, or other procedures.

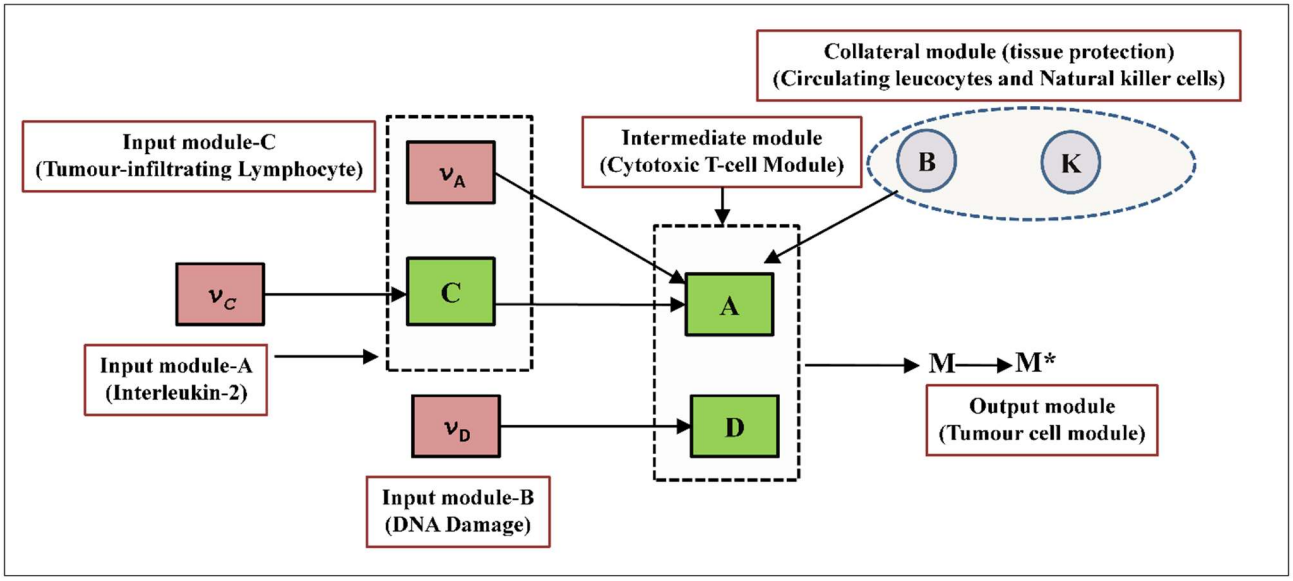

Figure 3. Computational systems analysis of activation of multimodal entities (Interleukin-2, Cytotoxic T-cells and DNA damage) which enables tumor eradication, endogenously or exogenously.

2.3. Formulation of extinction of tumor cells

We here represent the interaction of the different cellular populations in terms of the flowsheet in Figure 4. The details of the derivations of this section are furnished in [15]. Using primed symbols to denote temporal rates or time derivatives, we can formulate the temporal dynamical model, specifically the rate of change of concentration of IL-2 activation, as given in the equations below.

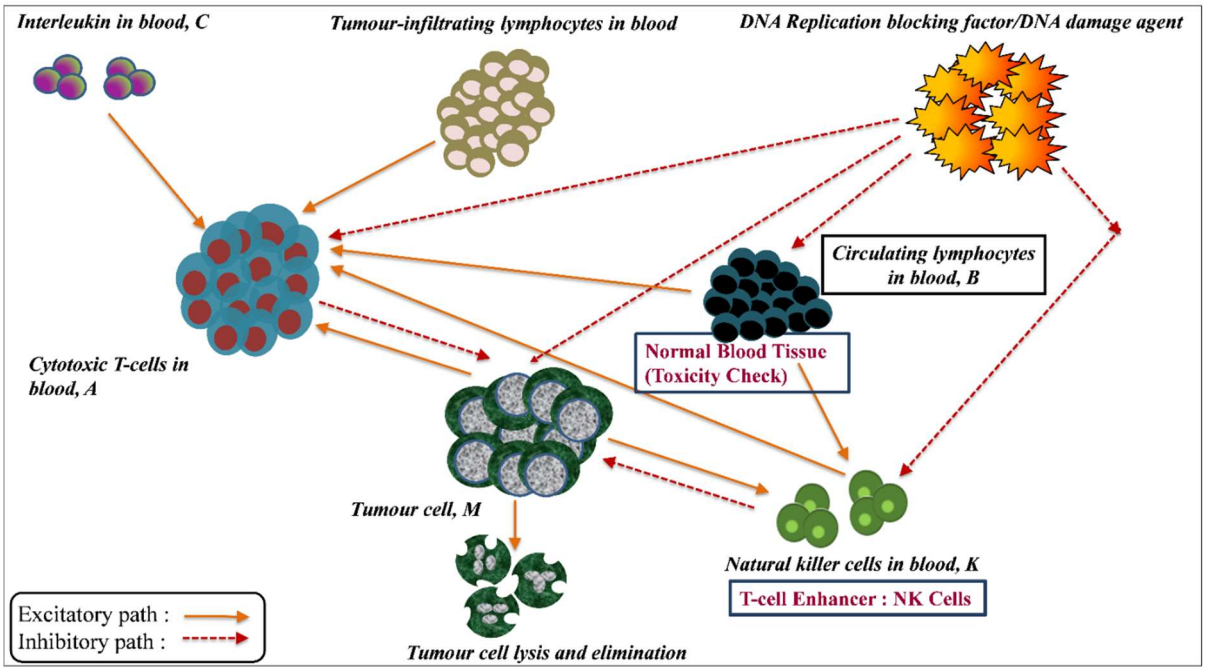

Figure 4. Interaction between the malignant lesion and the entities in its environment during endogenous or exogenous regression of the lesion (i.e., host-induced or therapy-induced regression).

(i) Interleukin:

$$C' = \underset{\text{Interleukin formation rate}}{\underbrace{v_C(t)}} - \underset{\text{Interleukin elimination rate}}{\underbrace{\mu_C C}} \tag{1}$$

where $v_C(t)$ represents the interleukin-2 formation in the system, and the interleukin degradation or elimination being according to the rate principle, i.e., proportional to its concentration, with μ_C being the decay rate. Similarly, we have the formulation of the rate of change of level of DNA interference:

(ii) DNA damage:

$$D' = \underset{\text{Generation rate of DNA blockage factor}}{\underbrace{v_M(t)}} - \underset{\text{Elimination rate of DNA blockage factor}}{\underbrace{\gamma D}} \tag{2}$$

where γ is the corresponding decay rate of the elimination or degradation of the DNA blockage factor. Likewise, we can formulate the dynamics of circulating white blood cells B:

(iii) Circulating leucocyte:

$$B' = \underset{\substack{\text{Birth of} \\ \text{circulating cells}}}{\underbrace{\alpha}} - \underset{\substack{\text{Death of circulating} \\ \text{cells (senescence)}}}{\underbrace{\beta B}} - \underbrace{k_B(1 - e^{-D})B}_{\substack{\text{Lysis of circulating cells} \\ \text{associated with DNA damage factor}}} \tag{3}$$

where the leucocytes are generated at rate α from marrow, and they age with a death rate β, while the last expression ($1 - e^{-D}$) is the saturation term denoting the fractional kill of these cells by the DNA blockage factor. After that, we formulate the natural killer cell dynamics:

(iv) Natural killer cells:

$$K' = \underset{\substack{\downarrow \\ \text{NK cell birth from circulating leucocytes}}}{eB} - \underset{\substack{\downarrow \\ \text{NK cell death by senescence}}}{fK} - \underset{\substack{\downarrow \\ \text{NK cell de-activation by tumor cell debris}}}{pKM} - \underbrace{k_K(1 - e^{-D})K}_{\substack{\text{NK cell lysis Associated with DNA damage factor}}} + \underbrace{g\frac{M^n}{h+M^n}K}_{\substack{\text{NK cell recruitment by tumor cells (Michealis-type)}}} \quad (4)$$

Here, the last expression $[KM^n/h + M^N]$ is a modified Michaelis-Menten type term, providing a saturation effect in cell-cell interactions, and g, h and n are three logistic constants ($n \approx 2$ here). Furthermore, we consider another saturation effect, the intensity Q of the interaction between tumor cells (M) and antitumor lymphocytes (A). Using another three logistic constants d, s, and l, we can elucidate Q as:

(v) Tumor cell–Cytotoxic T cell interaction:

$$Q = d\frac{(A/M)^l}{s+(A/M)^l} \quad (5)$$

$$\underset{\substack{\downarrow \\ \text{Saturation function}}}{}$$

(T cell – Tumor cell interaction: Michaelis-Menten (MM) type)

The cytotoxic T-cell dynamics can now be delineated as:

(vi) Cytotoxic T-lymplocyte (CTL) dynamics: $CD8^+$ T-cells:

$$A' = -mA + \underbrace{j\frac{(QM)^2}{k+(QM)^2}A}_{\substack{\text{T-cell recruitment by tumor cell (MM)}}} - \underset{\substack{\downarrow \\ \text{T-cell de-activation by tumor cell}}}{qAM} + \underbrace{(r_1K + r_2B)M}_{\substack{\text{T-cell activation by NK + circulating cells}}} - \underset{\substack{\downarrow \\ \text{T-cell suppression: NK cell dependent}}}{uKA^2} - \underbrace{k_A(1 - e^{-D})A}_{\substack{\text{T-cell lysis associated with DNA damage factor}}} + \underbrace{\frac{p_C\,AC}{g_C+C}}_{\substack{\text{T-cell stimulation by IL-2}}} + v_A(t) \quad (6)$$

where mA represents T-cell death (senescence), and the last term $v_A(t)$ represents Tumor infiltrating lymphocyte formation rate. Here the terms are explained by the captions beneath; the right-side's second term $[(QM)^2/\{k+(QM)^2\}]$ and second-last term $[(p_CAC)/(g_C + C)]$, are saturation effects in cell-cell interactions. Lastly, we formulate the tumor cell dynamics as:

(vii) Tumor cell dynamics:

$$M' = \underbrace{aM(1 - bM)}_{\substack{\text{Logistic tumor growth}}} - \underbrace{(cKM + QM)}_{\substack{\text{Tumor lysis by NK cell \& T cell}}} - \underbrace{k_M(1 - e^{-D})M}_{\substack{\text{Tumor cell lysis by DNA damage factor}}} \quad (7)$$

It may be mentioned that the right-side of Eqs (1)–(7) has several cellular parameters (such as a, b…, α, β…), and their symbols, numerical values, significance and references, are given in Table S1 of the Supplement.

2.4. Protection of normal host tissue

Note that DNA damage, whether endogenous or exogenous, induces lysis of the host's cellular populations: antitumor lymphocytes, natural-killer cells, and circulating leucocytes, the lysis rate parameters being respectively k_M, k_A, k_K, k_B in Eqs (3), (4), (6) and (7). However, tumor cells are more sensitive to the DNA damage lysis than other cells ($k_M > k_A$, k_K, k_B [33]). An important aspect here is that normal host cells should not be damaged appreciably and should be protected. This is taken care of by setting up limits that should not be crossed by the host system during the regression process since the host cell populations need to be maintained within a minimum and maximum value (upper and lower bounds). Too high a value of an entity can be toxic to the system, and the population of host cells that protect against infection (as circulating lymphocytes and natural killer cells) should be above a minimum value, whereby the normal tissue will be protected. The importance of the lysis parameters and limit thresholds for both endogenous and exogenous regression are described in Supplementary (Section 2.2). These values are displayed therein, in Table S2.

A fundamental prerequisite is that the regression process should take place in such a way that all the tumor cells are eradicated, but there should be least damage and cellular toxicity to the host. A measure of normal tissue damage due to the aforesaid antitumor entities (chemomodulation or immunomodulation) can be described by the standard toxicity cost functional J, wherein toxicity to the cell, a second-order mass-action effect [40]**,** depends on second-power of the intensity-level of the antitumor entity:

$$J = \tfrac{1}{2} \left(r_1 U_1^2 + r_2 U_2^2 + \ldots. \right) \tag{8}$$

where U_1 , U_2, …. are the levels or effects of different antitumor entities, while r_1 , r_2 , …. are the weighting factors of each of the various entities. For instance, in the case of endogenous tumor regression, the effect level of immunomodulation U_1 can be taken to be the intensity of tumor-cell lysis by cytotoxic T-lymphocyte, i.e., term Q in Eq (7), while the effect level of chemomodulation U_2 can be gauged by the intensity of tumor-cells lysed by the DNA damage factor, i.e., the last term $k_M(1 - e^{-D})$ in Eq (7). We use this least damage principle to probe the conditions of tumor regression that would be optimal for the system, producing the minimal damage to normal tissue.

2.5. Path of complete tumor regression process

As the tumor undergoes permanent regression as per the formulation in Eq (7), we now endeavor to find out the temporally-varying activation level of the five associated factors: interleukin C, DNA damage D, circulating leucocytes B, natural-killer cells K, and antitumor lymphocytes A. In other words, we need to solve the Eqs (1)–(7) using the boundary conditions that these biological antitumor parameters (C, D, B, K and A) do not cross the physiological limits or bounds, see first paragraph of this section above and also the Supplement (Section 2 and Table S2).

Through solution of the Eqs (1)–(7), we find the values of the five antitumor factors and their alteration with time, which are necessary for inducing the tumor to follow the temporal trajectory of

Figure 1(b), so that there is elimination of full tumor cell population at time t_F, of that figure. Solving the equations, we have following pattern of activation intensity of the factors that together produce the complete tumor regression. The description of the equations are first mentioned below, and then information is given on their derivation. These equations are:

(i) Temporally-varying pattern of the activation level of DNA damage for tumor extinction:

$$D(t)^{\ddagger} = -\,ln\left[\,1-\left\{b_M g_{M_1}/r_{M_1}\mathrm{G}\right\}\right] \tag{9}$$

where $D(t)^{\ddagger}$ indicates the required DNA blockage factor concentration in blood which enables the tumor to undergo complete regression by the extinction time t_F, [the duration t_F, is shown in Figure 1(b). Further, in the above equation, b_M denotes the combined tumor cell-killing effect of DNA blockage factor and cytotoxic T-cell lymphocytes. If b_M is negative, the tumor will have regression; if b_M is zero, the tumor becomes stable in steady state; and if b_M is positive, then the tumor is in progression phase. The parameters g_{M1} and g_{M2} are respectively the biological toxicity effect on normal tissue due to the DNA blockage factor and cytotoxic T-cell. The parameters r_{M1} and r_{M1} denote the toxicity weighting index respectively of DNA blockage factor and cytotoxic T-cell; these toxicity weighing indices are the weighing factors mentioned in Eq (8). The term G is the combined normalized toxicity weighting factor for both DNA blockage agent and cytotoxic T cells together, namely

$$\mathrm{G} = [(g_{M1}{}^2/r_{M1}) + (g_{M2}{}^2/r_{M2})] \tag{10}$$

(ii) Temporal pattern of cytotoxic lymphocyte activation for tumor extinction:

$$A(t)^{\ddagger} = -\left[sM^{l}\left(b_M g_{M_2}/r_{M_2}\mathrm{G}\right)/\left\{d-\left(b_M g_{M_2}/r_{M_2}\mathrm{G}\right)\right\}\right]^{1/l} \tag{11}$$

where $A(t)^{\ddagger}$ signifies the desired cytotoxic T-cell population in the blood which enables the tumor to undergo complete regression by time t_F. In Eq (1), the terms s, l and d are the tumor cell lysis parameters due to action of cytotoxic T cell on the tumor (explained in Table S1 of the Supplement). The parameters b_M, g_{M2}, r_{M2}, and G have already been explained in the above paragraph.

(iii) Temporal pattern of interleukin-2 activation for tumor extinction:

$$C(t)^{\ddagger} = \mathrm{g_C} b_A/\left(p_C A\, r_{A1} H - b_A\right) \tag{12}$$

where $C(t)^{\ddagger}$ represents the Interleukin-2 concentration in the blood which enables the tumor to undergo complete regression by time t_F. In the above equation, g_C denotes the steepness index of cytotoxic T cell recruitment by interleukin IL-2, and b_A is the total cytotoxic T cell activation effect induced by DNA blockage factor and autocatalytically by cytotoxic T cell. The parameter p_C is the maximum value of the rate of cytotoxic T cell recruitment by IL-2, and A represents the cytotoxic T-cell population. The terms r_{A1} and r_{A2} are the toxicity weighing factors denoting the toxicity effect on cytotoxic T cell due to both IL-2 and autocatalytically by cytotoxic T-cell respectively. The term H is related to the above-mentioned toxicity weighing factors r_{A1} and r_{A2}, namely

$$H = [(1/r_{A1}) + (1/r_{A2})] \tag{13}$$

The details of the aforesaid derivations have already been explained in our previous work [15]. However, in that work, we had neither formulated nor provided negative bias, and so there were some amount of residual malignant cells persisting. In contrast, in this present report, we have furnished our novel methodology of negative bias, and we thereby show that all malignant cells become extinct in the desired duration. Furthermore, our previous publication [15] was a mathematical derivation paper, there was absence of any biological, tissue-based, clinical or molecular biology analysis. In the current report, we have satisfactorily given all these biological and clinical findings for enhancement and validation of our new approach of tumor eradication under the novel approach of negative biasing.

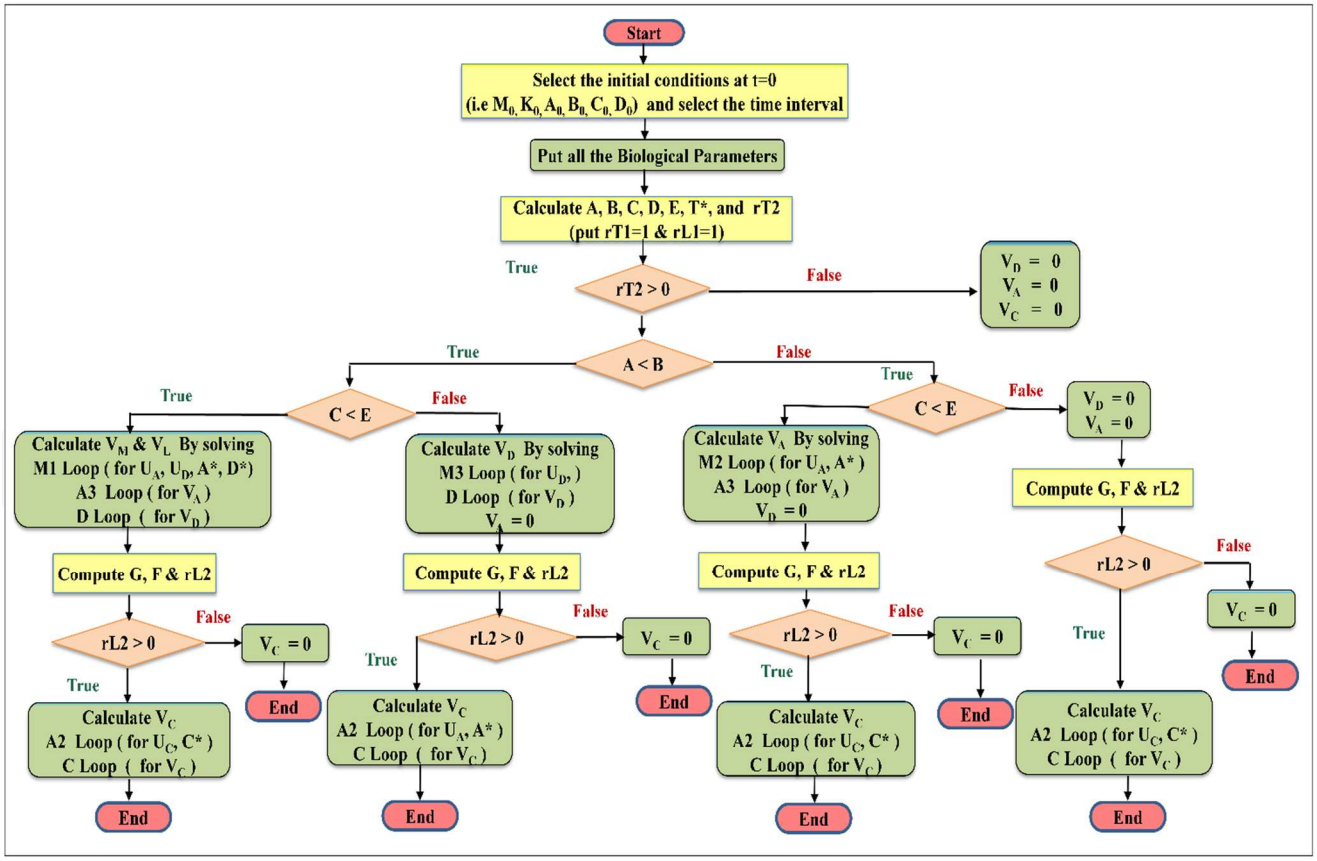

Figure 5: Flow chart for computational modelling of Endogenous or Exogenous regression of malignant lesion (i.e., Spontaneous tumor regression or Treatment-induced tumor regression respectively).

The parameters b_M , b_A , g_{M1} , g_{M2}, G and H depend on the value of the tumor characteristics (M, k_M ,k_A) and on the toxicity-minimizing indices (r_{M1}, r_{M2}, r_{A1} , r_{A2} ,) [15]; the other parameters in the equations (s, l, d, g_C, p_C) depend on the tumor growth and tumor lysis characteristics, having the values as in [33]. The temporal pattern of the circulating leucocyte population B and natural-killer cell population K, can be found by respectively solving Eqs (3) and (4), where we use the values of the relevant parameters which are also available [33]. The tumor cell population can be obtained as follows. We substitute these values of $C(t)$, $D(t)$, and $A(t)$ into Eqs (1), (2) and (6) and thus arrive at the values of Circulating leucocyte, NK-cells, and Cytotoxic T-cells. Then we put the latter three values in Eq (7) and thus obtain the value of the tumor cell population $M(t)$.

The quantitative formulation of our simulation model of endogenous or exogenous tumor regression is explained in Figure 5. We have used a Matlab platform to compute the profiles of the three entities (DNA damage, cytotoxic T-cell, and Interleukin-2), using tuning parameters values (rT2 and rL2) described in [15]. [Note that DNA damage events of endogenous regression are estimated in terms of equivalent alkylation activity of an alkylator agent (units of dacarbazine equivalents), as per Supplementary (section 2.1)]. For the initialization of the model, we have to provide initial intensity value of all the different cellular populations, i.e., their values at time point t_0 (at the beginning of tumor regression). After that, we need to provide all the biological parameters used in Eqs (1)–(7) [33]. Thence, we need to calculate the negative bias value (M*) and set the tuning parameters (rT2 and rL2). The tuning parameter rT2 is used to calculate the control parameter v_A and v_D, and the tuning parameter rL2 is used to calculate v_C [15].

Here we have divided the profile of the three entities (DNA damage, T-cell, and IL-2) in 4 loops (M - Loop, A- Loop, D - Loop and C - Loop) as elucidated in [15]. M-Loop is again divided into 3 loops M1- Loop used to calculate value of U_A, U_D, A*, and D*, M2- loop is for the calculation of U_A and A*, and M3-loop is for U_D and D* (note that here U_A and U_D indicate the anti-tumor behavior of cytotoxic T-cell and DNA damage respectively). Similarly, A-loop is again divided in 3 loops; A1-Loop is used to calculate value of U_C, v_A, and C*, A2- loop is for the calculation of U_C and C*, and A3-loop is for v_A calculation alone (here U_C denotes the anti-tumor behavior of IL-2). At last, the D-loop and C - loop is used to calculate v_D and v_C dose rates according to Figure 3. In other words, initially, the curve of tumor decreases and extinction is formulated by allotting a desired suitable extinction time t_F (this gives the negative bias M*, Figure 1(b)). Then the modelling is performed, whereby the aforesaid methodology and algorithm above will simulate the tumor regression process, so that the tumor cell population follows the extinction process of Figure 1(b). The moment the simulation gives the tumor cell population as a (small) negative value, the procedure will convert the negative value to zero (the tumor cells have become extinct before attaining a negative value). From this time point onwards, the simulation procedure will maintain the tumor cell population at 0 henceforth, and so there will be no tumor relapse. Thus, the simulation process will give (for each time step) the levels of DNA damage, cytotoxic T-cell, and Interleukin-2, whereby these three entities jointly gradually eradicate the tumor cell population by time t_F.

2.6. Validation of the computational model using experimental biological system

The mathematical model is verified on immunohistochemical experiments and microarray assay of a preclinical model of permanent spontaneous tumor regression in melanoma. Here, numerous tumors appear in pigs, they grow rapidly for the first 1½ months, and then spontaneously regress completely by 3–4 months in half of the animals, but in the other half, the tumors spread and kill the animals [24]. In the study, six pigs who went into the regression mode, were investigated, tumors had biopsy under anesthesia at three weekly intervals across three months, at these five different time points as follows, t_0 = day-of-birth (d) + 8 days after birth (i.e., $d + 8$), thence $t_1 = d + 28$ days; $t_2 = d + 49$; $t_3 = d + 70$, and $t_4 = d + 91$ (Schema-2). At each time point 5–6 tumor-masses were biopsied, and subjected to microarray investigation using Ingenuity algorithm.

Time					
Weeks:	1	4	7	10	13
Days	8	28	49	70	91
Time-span (%)	8.8%	30.7%	53.8%	76.9%	100%

Schema-2. Temporal sequence of tumor biopsy analysis across the tumor regression process.

(i) Pre-clinical investigation

Regarding the aforesaid melanoma regression analysis, we accessed the gene expression profiles of E-MEXP-1152 from the ArrayExpress facility (https://www.ebi.ac.uk/arrayexpress/) [41]. The microarray assay was based on Transcription profiling of tumor from the melanoblastoma-bearing Libechov Minipig (MeLiM) model and the Porcine Genome Arrays platform. This involved 5 different tumors of 5 pig siblings, each across 5 time points, from day 8 to day 91 after birth (Submission date: September 10, 2008). Also, the time-dependent gene expression profiling of the spontaneously regressing melanoma tumor biopsies was performed. Further, from the ArrayExpress platform, we analyzed all the raw information CEL-Files (E-MEXP-1152.raw.1.zip) belonging to this experiment (https://www.ebi.ac.uk/arrayexpress/experiments/E-MEXP-1152/).

(ii) Normalization and statistical analysis

We then performed normalization, statistical analysis and the analysis of variance (ANOVA) of the microarray information, using R platform and Bioconductor statistical facility (http://www.bioconductor.org/) [42]. We did the preprocessing step utilizing the GeneChip Robust Multiarray Average (GC-RAM) method to get the gene expression matrix from Affymetrix information. For identification of differentially expressed gene in log_2 scale, we used the Transformation for t-test and one-way ANOVA. Thence, differentially expressed Probe sets were selected on the bases of p value and fold change (FC) value [(FC) > 2 and p value < 0.05]. Moreover, the significant probe sets after ANOVA were used for biological functional analysis and comparison.

(iii) Time dependent biological function analysis using pathway study

We then identified the temporal profile of the microarray data for the different Biological Classes category, utilizing the Ingenuity Pathway Analysis procedure (IPA). We also elucidated the expressional changes at each time-point, the functional interpretations, and the biological interaction of the genes, which were also demarcated using IPA. This furnished the temporal pattern of gene-expression levels corresponding to the effector components of Figure 4, such as (i) DNA damage (G2/M checkpoint regulation), (ii) Antitumor lymphocyte activation (T-lymphocyte Receptor Signaling), Natural Killer cell activation (NK signaling), etc. We also clustered the genes corresponding to different canonical pathways utilizing IPA methodology, out of these genes we identified the most significant genes with high FC-value.

3. Results

We first obtained the inferences from the computational modelling analysis developed above. Then we furnished experimental findings from the preclinical studies, to validate the theoretical quantitative formulation.

3.1. Mathematical modelling and computational simulation for tumor regression model

We have used the MATLAB platform to numerically solve the Eqs (1)–(7), and find the values of these parameters and their alteration with time, while the tumor follows the temporal trajectory of Figure 1(b); the complete flow-chart is shown in Figure 5 and the simulation has already been described in the "Materials and methods" Section, item 2.5.

3.2. Tumor system behavior

Here we deal with an indicative case of melanoma. Melanoma is a neural crest cell tumor and shares many similarities with common neural system tumor as glioma. We can take the initial realistic situation as starting malignant cell population (T_0) of 2×10^7 cells, natural killer cell population of 10^5, cytotoxic T-cell population of 5×10^4, and circulating lymphocytes of 10^9. These realistic values are adapted from an earlier analysis of tumor dynamics [33]. The number of tumor cells corresponds to a realistic tumor which has just been radiologically detected, say a metastatic melanoma mass in the liver (radiological detection threshold ≈ 1 cc. tumor, having 10^7 malignant cells [43]). All the other constants used in the model are given in [33], with the tumor cell growth rate, $a = 0.301$ per day, and the deceleration rate of logistic tumor growth $b = 1.01 \times 10^{-8}$. Here, we have considered a more aggressive melanoma tumor, so the tumor cell growth rates a can be taken to be 50% higher of the aforesaid a value (i.e., new value of a is now 0.43).

To be able to compare endogenous and exogenous regression in a common platform, we need to estimate the DNA blockage in both endogenous and exogenous tumor regression using a common unit, we have formulated this common unit as an equivalent unit of alkylation blockage activity (i.e., in terms of alkylation activity of equivalent amount of chemotherapy dacarbazine which will produce the same number of DNA blockage events either in exogenous or endogenous regression of tumor) (Section 2.1 of the Supplement).

(i). Tumor regression under conventional therapy (without Negative Bias): Tumor Relapse

We now formulate the case of a conventional protocol of chemotherapy and immunotherapy of melanoma, utilizing (i) Chemotherapy: Six pulses of chemotherapy, one every 10 days (dacarbazine 5 mg/kg/day pulse), (ii) Interleukin-2: Six pulses of 500,000 i.u/kg/day, from day-8 to day-11. (iii) Cytotoxic T-cells: Total 10^9 cells during an infusion at day-7 through day-8. We have applied these values to the initial Eqs (1)–(7) which are solved to obtain tumor cell population M as time elapses. Figure 6 shows that the tumor cell population initially decreases to about 100,000 malignant cells, but later manifests as cancer relapse and increases to high values (≈10^9 malignant cells) that corresponds to a large tumor of diameter ≈6 cm., such a tumor will have penetrated the blood vessels, producing wide dissemination and lethality.

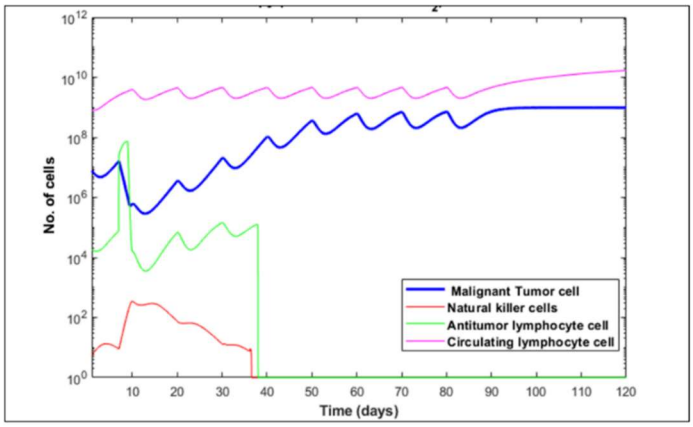

Figure 6. Conventional treatment protocol using chemotherapy and immunotherapy. This uses DNA blocking alkylator drug dacarbazine, and immunotherapy (Cytotoxic T-lymphocyte and Interleukin-2). The protocol fails to eliminate malignant melanoma tumor cells, and after treatment duration there is relapse of the malignancy.

(ii). Tumor regression by negative bias formulation: Permanent tumor elimination

Here we have used the different sets of Eqs (9), (11) and (12), which give the levels of the three entities (DNA damage, cytotoxic T cells, interleukin-2) that are required to enforce the cell population of the melanoma tumor to follow the exponentially declining trajectory to zero cell at a specific desired duration (46 days). We now simulated the equations at a time-step of a 0.01 second, and obtain the values of the levels of DNA damage, Interleukin-2, and Cytotoxic T-cells, which would enable the tumor population to follow the targeted diminishing curve trajectory of Figure 1(b), aimed at tumor extinction in 46 days. These levels of the above three entities are then used to obtain the tumor cell population (using the other set of Eqs (1)–(7)). Therein, the populations of the circulating leucocytes and natural killer cells are also calculated. Note that the actual tumor cell population obtained (Figure 7(a)) follows in principle the desired exponentially decreasing trajectory that we planned, whereby all tumor cells undergo eradication. Note that none of the system parameters (DNA damage level, circulating lymphocytes, NK cell, cytotoxic T-cells) crosses the respective upper and lower physiological bounds or thresholds of Table S2 (Supplement), thereby ensuring normal tissue protection. Here, we found the negative bias to be $M^* = 1.8986 \times 10^5$ cells. Since the total number of initial tumor cells $M_0 = 2 \times 10^7$ cells, we observed that the relative value of M^* is small, at about 1% of the initial tumor load.

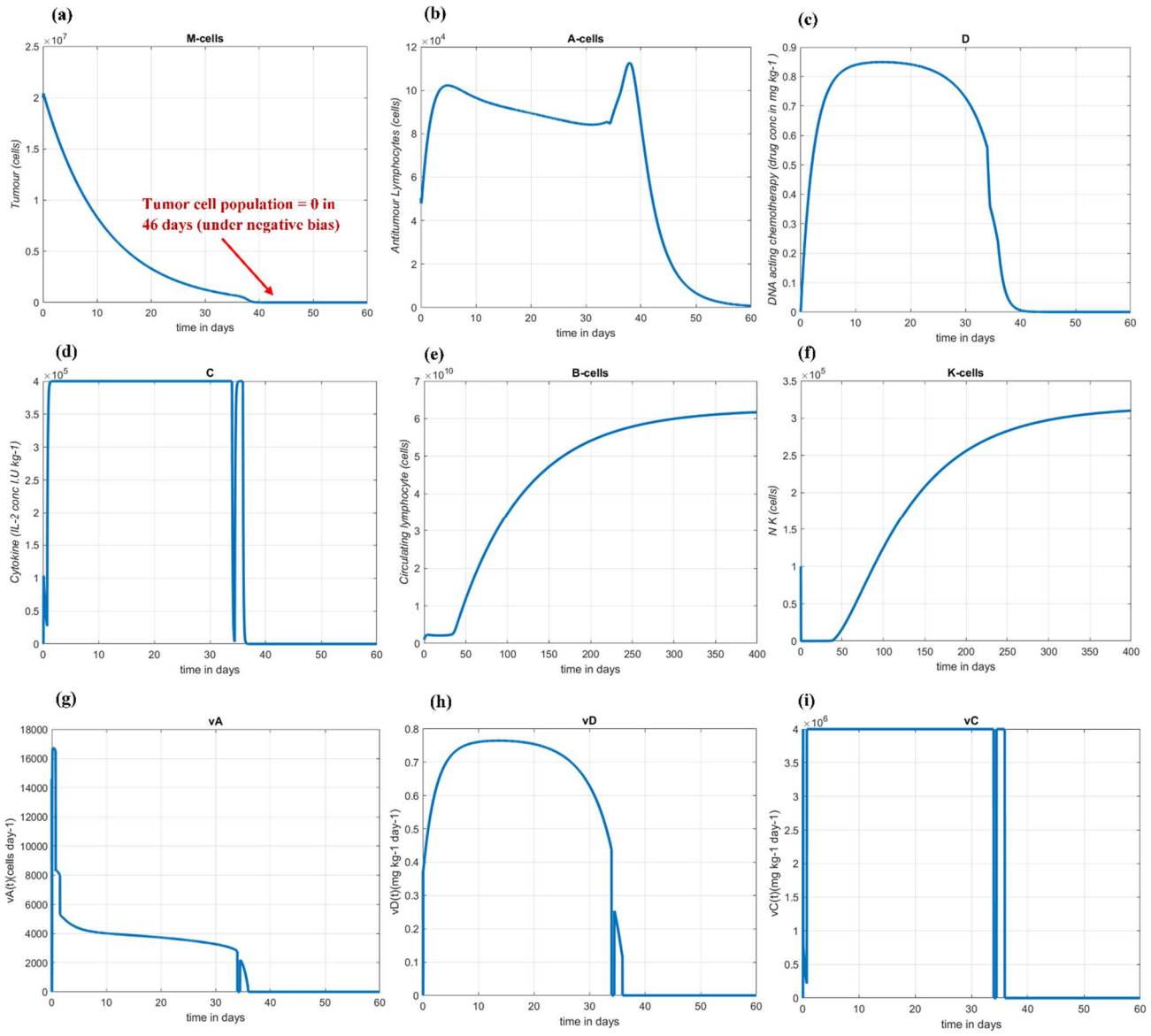

Figure 7. Complete elimination of melanoma tumor under negative bias. (a) Consistent decline of tumor cell population with time: Complete elimination of tumor at 46 days by following negative biasing behavior of Figure 1(b) scheme. (b) Bimodal temporal profile of cytotoxic T-cell required for eliminating Tumor cells. (c) Unimodal profile of level of DNA damage required for eliminating Tumor cells (DNA damage is estimated in terms of equivalent amount of alkylator substance dacarbazine that produces similar amount of DNA damage, see text). (d) Concentration profile of Interleukin-2 required for tumor elimination (the curve displays a stationary level). (e) Temporal profile of circulating lymphocyte level required for tumor elimination (the curve levels off at a saturating value). (f) Temporal profile of natural killer cell level required for tumor elimination (the curve levels off at a saturating value). (g) Interleukin-2 input rate that would enable tumor elimination. (h) DNA blockade input rate that would enable tumor elimination (estimated in equivalent amount of rate of input of alkylator substance dacarbazine). (i) Tumor-infiltrating lymphocyte input rate that would enable tumor elimination.

(iii). Behaviour of cancer stem cells, natural killer cells and circulating lymphocytes

From Figure 7(e),(f), we see that the population of circulating lymphocytes and natural killer cells in the body attain the values respectively of 6×10^{10} cells and 3×10^{5} cells, which are very much below their corresponding upper bounds, and are only about 10 and 0.001% of the respective upper bounds in Table S2 (Supplement). Furthermore, it is known that cancer stem cells become much resistant to anti-tumor drugs as they have drug efflux channels which ejects out the drugs from the tumor cells. For instance, the sensitivity of the cancer stem cells to a drug can become 8–23% of the sensitivity of general cancer cells to that drug [44], this drug sensitivity of tumor cell is the parameter D in Eq (2). Hence, to formulate cancer stem cells in the model, we decrease the drug sensitivity D to 1% of the value that we have used in the earlier paragraph, this very low value of D has been put as a precautionary measure. We performed the simulation of the earlier paragraph again, and we observed that there is also complete tumor eradication (Figure 8), though a somewhat longer therapy duration is needed (59 days). Thus, our negative bias procedure can successfully eliminate the cancer stem cell base in the tumor, though the time taken is a little longer.

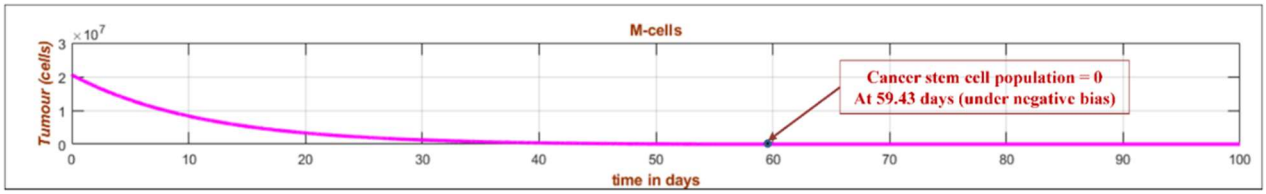

Figure 8. Complete elimination of cancer stem cells. The tumor will need more time for the cancer stem cells to be extinct (in 59 days) with chemotherapy sensitivity at 1% of usual cancer cells.

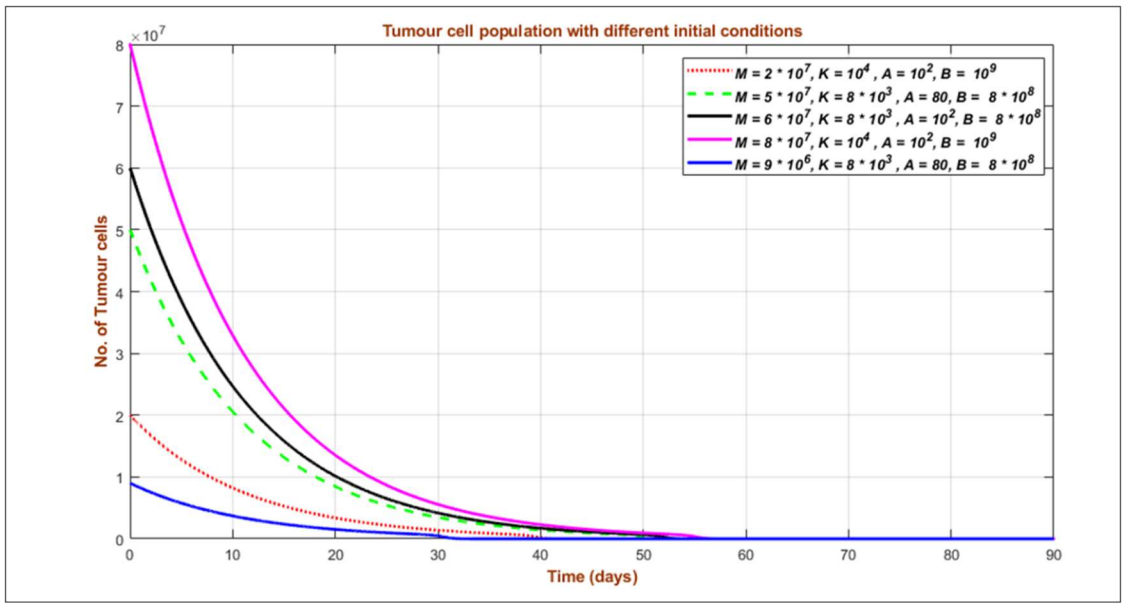

Figure 9. Decrease of tumor cells population with different initial conditions. Extinction of the tumor occurs regardless of the initial conditions.

(iv). Adaptability and robustness of tumor elimination process

In real-life conditions, different patients can have different initial conditions and constitutions. Hence, different patient-specific initial situations are now considered, for example, we examined the different initial condition of immunological system (like populations of the different effector cells) and carried out 500 arbitrarily simulations for complete tumor elimination for melanoma tumor with different biological parameters or characteristics (Figure 9).

We found that tumor extinction occurred in 100% cases if the coefficient of variation in effector cell population was 0%, while extinction happened in 98% of the cases if the coefficient of variation was increased to 10%. It has been known that the physiological parameters are generally kept constant homeostatically by organisms, with a 10% variation around the mean level [45]. Thus, within the considered range of physiological variation, it transpires that our proposed approach may be able to induce tumor elimination in the majority of the cases (98% of cases).

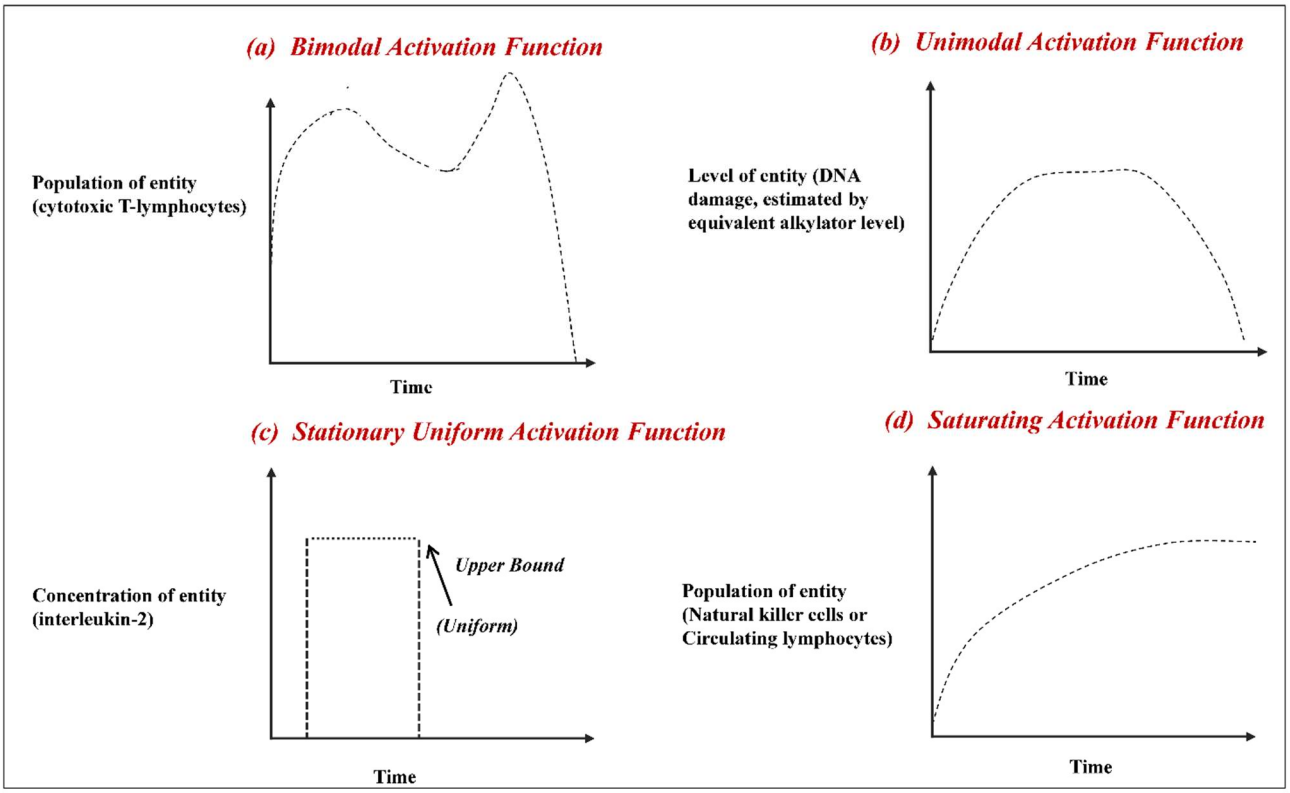

Figure 10. For complete regression of tumors with different initial conditions, the time-wise alteration of the tumor-affecting entities involved does follow the common pattern template: (a) Bimodal intensity of Cytotoxic T-cell, (b) Unimodal intensity of DNA blockade factor, (c) Uniform stationary intensity of Interleukin-2, (d) Saturating intensity of Natural killer cells and Circulating lymphocytes.

(v). General characteristics of tumor regression process

We have simulated the permanent tumor regression process using different values of the tumor parameters, and we have always observed the similar type of patterns as in Figure 7. This general

pattern is exhibited in Figure 10, whereby we note that for inducing permanent tumor regression, the three antitumor entities should have three distinct temporal profiles (tri-phasic activation):
1) Bimodal intensity for lymphocyte activation, showing two temporal peaks (Figure 10 (a)),
2) Unimodal intensity for activation of DNA damage (such as strand blockade or alkylation), displaying one peak temporally (Figure 10(b)).
3) Stationary intensity for cytokine activation (interleukin-2) exhibiting uniform level (Figure 10(c)).

(vi). Basis of the tri-phasic activation

The three aforesaid activational phases can be accounted for from a dynamic perspective of Figure 11. Initially, in the tumor cell surroundings, there occurs tumor cell antigen binding to T-lymphocyte receptor, stimulating the secretion of IL-2 (event-1). Thereby, T-cell is activated to cytotoxic T-cell (event-2). This T-lymphocyte then counters a tumor cell, secretes granzyme protease, which binds to tumor cell DNA, cleaving the nucleic acid binding protein, blockading the DNA and damaging tumor cell DNA replication (event-3). Note that in event-1, since there are no second-order deceleration terms nor Michelis-Menten terms in Eq (1), the interleukin level can rise rapidly or steeply, nevertheless the increase of interleukin halts or saturates as soon as the interleukin toxicity level or upper bound is reached.

The aforesaid three sequences of events are clearly reflected in the three temporal profiles above. The first event corresponds to Interleukin-2, the earliest agent to increase (Figure 10(c)). Then, the second event correlates with cytotoxic T-cell increase, but sometime later (Figure 10(a)). Thereafter, the third event relates to the increase of tumor cell's DNA damage intensity, which happens still later Figure 10(b). Here, tumor cells are increasingly lyzed, and their debris thus produced deactivates the cytotoxic T-cells whose activated population hence decreases, this corresponds to the negative term "-*qAM*" in Eq (6). As tumor cell population continues to decrease, its debris production falls, so that the negative term becomes smaller, whereby cytotoxic T lymphocyte population increases again (second temporal peak) (Figure 10(a)).

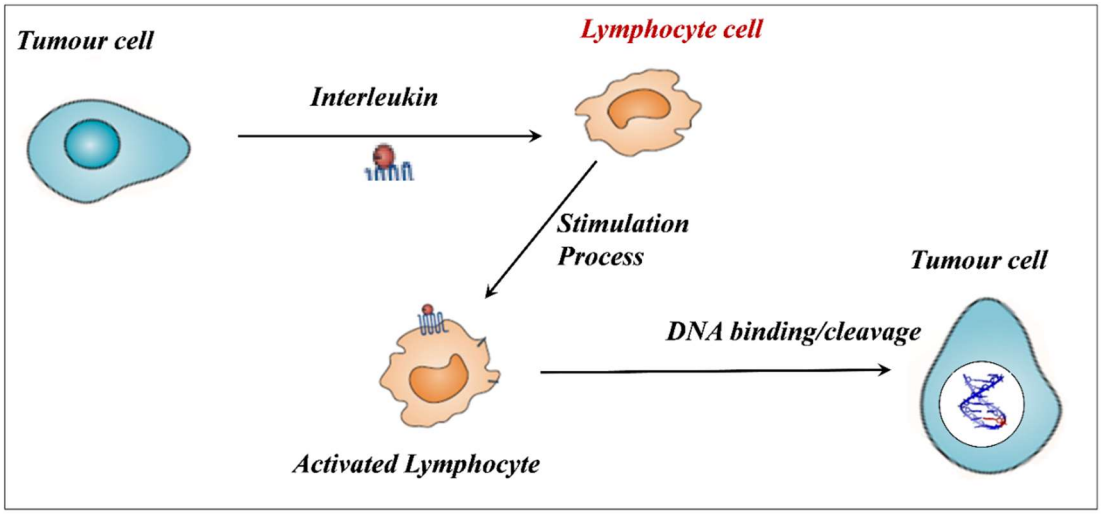

Figure 11. Basis of the tri-phasic activation process in tumor regression as illustrated by the three temporal transitions.

We may recollect that the step-like shape and stationarity in the interleukin-2 concentration is due to its level being initiated rapidly at the requisite intensity (Figure 10(c)). Such a brisk interleukin response has also been independently observed in the immunological system, where requisite stimulation can enable interleukin-2 receptor activation to reach substantial intensity within 2-4 days [46]. The result is that a stationary level of interleukin activation is rapidly attained, and tumor regression occurs. Indeed, it is well known from clinical experience [32], that interleukin-2 administered at significantly augmented dose, induces long-lasting immunomodulation to act against those residual malignant cells that bypass usual therapeutic intervention.

3.3. Experimental validation

We now furnish experimental findings of complete permanent tumor regression that provide substantiation and corroboration to our mathematical theoretical model of complete elimination of tumor by *the five-pattern temporal profile* (Figure 10*)*, namely the activation of antitumor lymphocyte (bi-modality), DNA damage or impairment (unimodality), interleukin-2 (stationarity), circulating lymphocyte (saturation) and NK cell (saturation).

3.3.1. Malignant melanoma elimination

(i) Melanoma microarray data preprocessing:

The microarray raw data of file of the spontaneous regression of malignant melanoma tumor was downloaded from the ArrayExpress system (E-MEXP-1152) and analyzed using the Bioconductor package on the R platform. Furthermore, one-way ANOVA was performed for five different time points (taking time t_0 as the reference) to find the differentially expressed genes based on p value and FC value (p value < 0.05 and FC > 2). The ANOVA analysis results showing the differentially expressed genes (DEGs) is displayed in Figure 12.

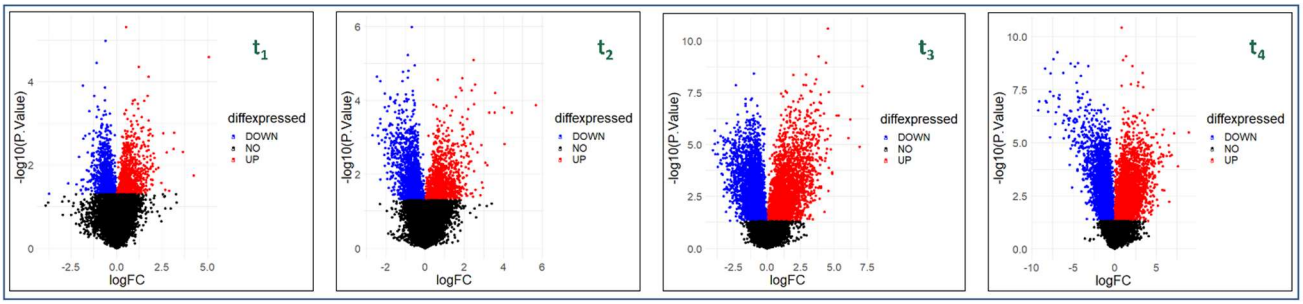

Figure 12. Volcano plots for differentially expressed genes. ANOVA analysis results showing DEGs plot: blue color signifies the downregulated genes, red color signifies the upregulated genes, and black color signifies the non-significant genes.

(ii) Identification of signaling pathways:

Permanent endogenous melanoma regression microarray data of pigs were investigated by IPA. We assessed the antitumor T-cell activation intensity by the level of the IPA's T-cell pathway, named "PD-1/PD-L1 cancer immunotherapy pathway". Similarly, we gauged the DNA impairment level by the IPA pathway "G2/M DNA Damage Checkpoint Regulation". Likewise, we estimated the Natural-Killer cell level by IPA pathways "NK cell signaling". Furthermore, we assay the Circulating lymphocyte level by the IPA pathway ("Leucocyte extravasation signaling"); indeed, one knows that during immune response, the extravasation of circulating leucocyte through the vascular wall into tumorous tissue, correlates with activation of circulating lymphocytes [47].

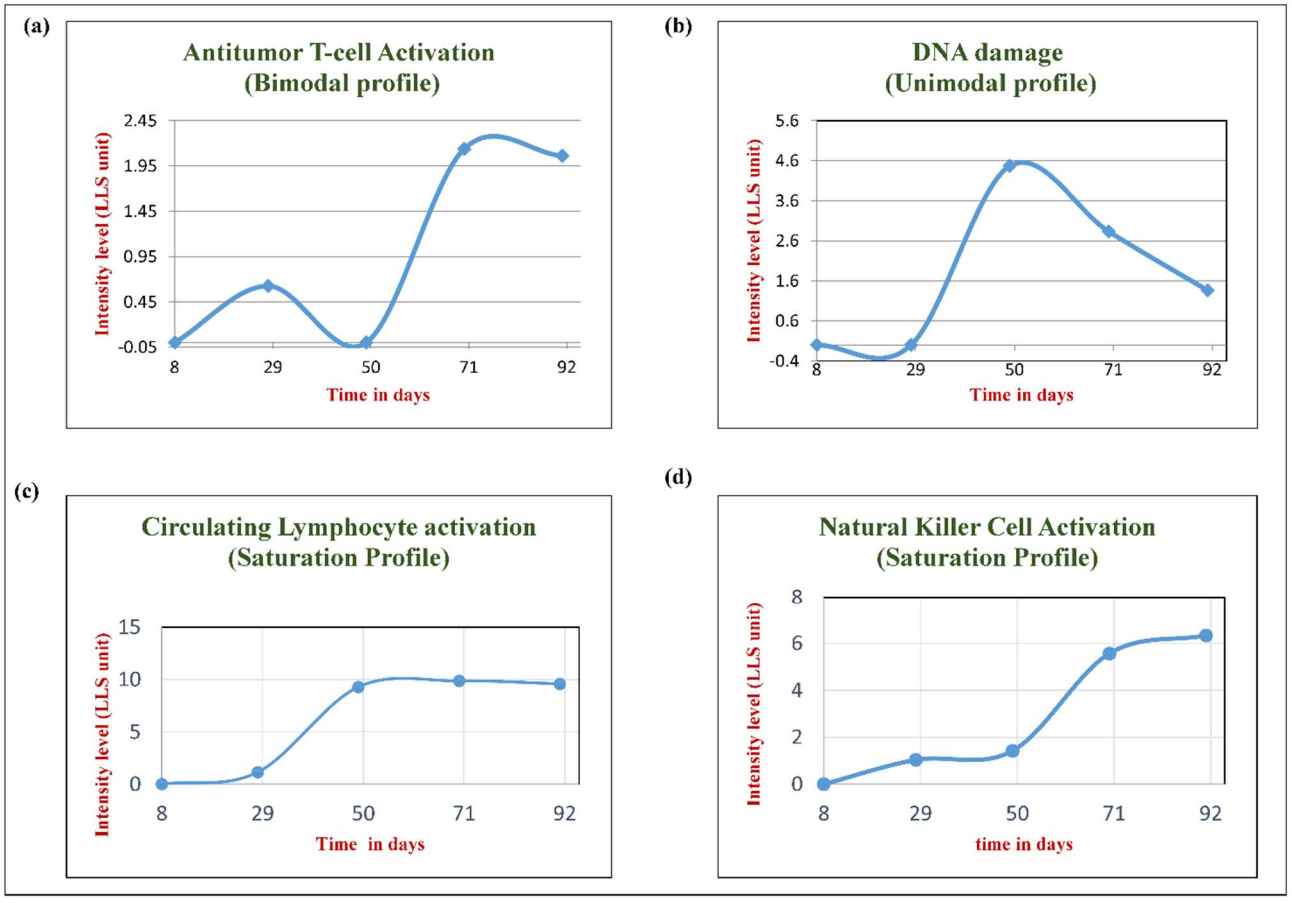

Figure 13. Comprehensive experimental validation of the prediction of the computational model. Behaviour of the various formulated entities needed for malignant tumor regression (melanoma) are shown, the entities being antitumor T-cells, DNA damage, Circulating lymphocytes, and Natural killer cells. (a)–(d) Activation of the biological readouts obtained using microarray data of the respective tissues at the various time-points, the vertical *y*-axis is in LLS units, i.e., log level of significance (i.e., *–log* (*p*-value)). Regarding the four curves, it is evident that their activations are respectively of bimodal (panel (a)), unimodal (panel (b)), and saturation patterns (panel (c), (d)), which are also predicted by our computational model developed theoretically for tumor regression (patterns of the computationally predicted theoretical curves are in Figures 7 and 10).

Thus, we found the specific temporal behaviour of the activation levels of cytotoxic T-lymphocytes (Figure 13(a)), DNA impairment (Figure 13(b)), circulating leucocytes (Figure 13(c)), and natural killer cells (Figure 13(d)). It is evident that the first and second curves (Figure 13(a, b) follow respectively the bimodality and unimodality pattern of Figure 10(a,b). Also, the third and fourth curves (Figure 13(c, d)) both follow the saturation pattern of Figure 10(d). Thus the four experimental curves of Figure 13 closely correspond to the mathematically predicted patterns of Figure 10.

To show that our theoretically calculated model of tumor regression (Figure 7) adequately describes the experimentally observed tumor regression behaviour (Figure 13), we used the goodness-of-fit criterion (Kolmogorov-Smirnov test). Accordingly, we found that the experimental graphs of panels (a)–(d) of Figure 13 are satisfactorily accounted respectively by the corresponding theoretical graphs of panels (b, c, e, f) of Figure 7, and the corresponding goodness-of-fit Kolmogorov-Smirnov's statistical test was satisfied ($\alpha = 5\%$).

Now, we arrive at the molecular biological basis of aforesaid biological entities involved in permanent endogenous tumor regression. Using genetic analysis, we also found the genes associated with these different entities, which we elucidate below. Table 1 (left three columns) summarizes the main aspects of our findings.

(iii) *Identification of genes*

We found the signaling pathways and related genes for spontaneous regression using IPA. We selected the gene based on FC-value from the cluster of gene obtained from IPA, for different biological classes. Accordingly, we have furnished below the two lead exemplar genes for the antitumor functions as follows (also see Table 1, right two columns):

(a) DNA Damage-related genes: *CDC2, CHEK*;
(b) Interleukin-2 signaling-related genes: *IL2RG, AKT3*;
(c) Natural-killer cell signaling-related genes: *NKG2D, KLRK*;
(d) Cytotoxic T-cell activation-related genes: *TRGV5, CD28*;
(e) Circulating lymphocyte activation-related genes: *TCA, CCL5*.

Table 1. Biologically-based experimental corroboration of the computed activation functions of the antitumor entities which enable complete tumor elimination: The characteristic computed functions [Eqs (1)–(4), (6)] are in the first column, rows 2–6), and for each of these functions, their corresponding biological significance and relationships are provided in the other columns. The negative bias function is also included as row 7).

Characteristic function predicted by mathematical model	Biological entities involved	Biological basis of the characteristic function	Exemplars of genes involved in the antitumor characteristic	Illustrative findings
Monophasic Activation (DNA blockage)	DNA. Chemomodulation: Cell multiplication blockage.	Build-up and then decay of DNA chemomodulative or blockage activity.	Cell kinase gene: *CDC2, CHEK1* Cell cycle gene: *CCNB1, CCNB3*	Figure 7(c), Figure 13(b)
Biphasic activation (Cytotoxic T-cell)	Lymphocyte enhancement: Lysis of tumor cells.	Second rise (biphasicity) in T- cell population due to decline of chemomodulation, i.e., decrease in blockage of T-cell growth.	T-cell receptor activation: *TRGV5* gene, CD28 gene. G-protein coupled receptor activation: *CALCR* gene, CBLB gene.	Figure 7(b), Figure 13(a)
Uniform Stationary activation (Interleukin-2)	Cytokine enhancement: Escalating the leucocyte-tumor cell interaction.	Toxicity limit of cytokine (homeostasis).	Interleukin-2 receptor gene: *IL2RG, AKT3* gene. Transmembrane protein: *CD74, GRB2* gene.	Figure 7(d), Figure 14(a)
Saturating Activation (Natural killer cell)	Natural killer cell function (normal tissue protection).	Equilibrium state after Tumor regression.	NK cell activator gene: *NKG2D* gene, *STAT4* gene Actuates NK cell function activators: *KLRK1* gene, *MAP3K12* gene.	Figure 7(f), Figure 13(d)
Saturating Activation (Circulating lymphocyte)	Circulating lymphocyte function (host defense).	Equilibrium state after Tumor regression.	Chemokine ligand 1 activity: *TCA* gene - Actuates lymphocytes & monocytes. Rantes ligand activity: *CCL5* and *PRKCB* genes - Actuates lymphocyte & monocytes.	Figure 7(e), Figure 13(c)
Negative biasing	Apoptosis pathway	Elimination of residual tumor cells.	Extrinsic apoptosis pathway activator genes: *CASP7* gene, *GZMB* gene. Intrinsic apoptosis pathway activator gene: *BCL2L1* gene	Figure 1(b), Section 3.3.1 (iv)

(iv) Negative bias related genes: CASP7, GZMB.

Now, for identifying the genes that function as effecting the negative bias in tumor cell reduction trajectory, we have selected the genes which are responsible for the apoptosis process of the tumor cells, namely the Perforin/Granzyme apoptosis pathway activator genes: *CASP7, GZMB*. In other words, the pathway is a serine protease pathway, which is a primary signaling route used by cytotoxic T cells and natural killer cells to eliminate virus-infected or mutated malignant cells [48]. Cytotoxic T cells have perforin, which is a pore forming complex, while Granzyme B (GZMB) is an apoptotic signaling molecule that is able to initiate apoptotic signal by the process of exocytosis. After getting into the mutated malignant cell, this GZMB molecules interact with BID protein of the cells, which is actually the BH3 interacting domain death family protein that initiates the apoptosis process by activating caspase 7. As shown in Table 2, the expression values of these two genes (*CASP7* and *GZMB*) increased from time point t_1 through t_4, while the tumor regression process advanced with time and this regression process was maximum at t_4 time point (where the tumor has completely regressed and become extinct). Indeed, the aforesaid proteins actuated by these two genes were able to attack and lyze all the residual tumor cells in the last time segment (t_3–t_4), thereby preventing tumor relapse.

Table 2. Genes inducing Negative bias with their activity values at different time points.

Gene Name	Log_2FC value (at time t_1)	Log_2FC value (at time t_2)	Log_2FC value (at time t_3)	Log_2FC value (at time t_4)	*p.* value	*F*	Average Expression
GZMB (Granzyme-B)	−0.07314	0.525236	1.124219	2.326586	0.00011	10.0495	6.086244
CASP7 (Caspase-7)	−0.02369	0.12626	0.570303	1.488125	0.03849	4.8372	7.215214

3.3.2. Malignant histiocytoma elimination

Here complete endogenous regression of malignant histiocyte tumor in rodent system was analyzed. The experimental investigation is available, along with biochemical parameters [49]. In Figure 13 we delineated the temporal behaviour of the relevant parameters, which we have calculated from that initial study. The experimental study was done for 32 days, and two types of tumor regression regimes were observed: (i) Early regressor animals, where tumor size increased up to the 10^{th} day, then tumor regression occurred, (ii) Late regressor animals, who display tumor size increased till about the 20^{th} day, and tumor regression started thereafter [49]. Hence, to observe the tumor decline process for a substantial duration, we analyzed the findings of the first group, where regression deviation was observed longer, namely across 22 days (in the second group, the regression duration was much shorter, only for 12 days). We note that the experimental graphs showing temporal profile of interleukin-2 and DNA impairment (Figures 14(a,b)) are satisfactorily described by the corresponding theoretical graphs predicted (Figure 7(d,c)), the Kolmogorov-Smirnov statistical test of goodness-of-fit being also satisfied ($\alpha = 5\%$).

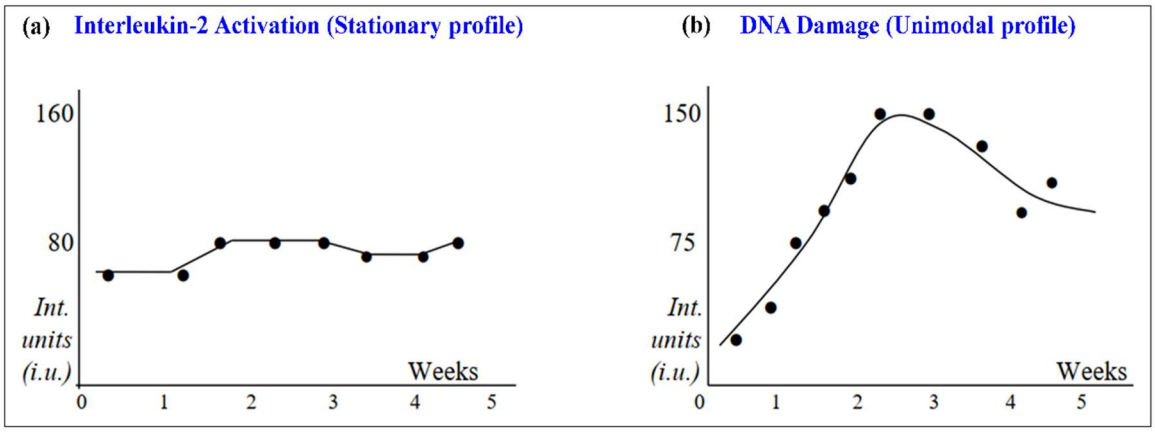

Figure 14. Permanent regression of malignant tumor: Empirical confirmation of the activation functions of the computational model, the tumor being malignant histiocytoma. (a) Interleukin-2 level as tumor regression ensues across time: the activation level is practically stationary. (b) Intensity of DNA damage, as gauged by level of TNF-α that induces DNA strand breaks. Note that here the activation function is unimodal.

4. Discussion

We have developed a quantitative mechanistic formulation and analysis of the permanent spontaneous regression of the malignant tumor, with experimental validation and its clinically-relevant implications. This extinction of tumor cells is possible due to a negative biasing process. We have delineated the temporal profile of the causative factors that enable the complete extinction of the tumor, namely:

(i) the three separate activation characteristics (unimodal, bimodal and uniform stationary activation function) respectively of DNA damage or mitosis blockage, cytotoxic lymphocyte and cytokine IL-2

(ii) the two separate saturation activation profiles of both the natural killer cells and circulating lymphocytes.

This multiphasic temporal orchestration of the antitumor entities minimizes toxicity to normal tissue, without damaging the usual host tissue. Furthermore, we have also obtained experimental corroboration of our theoretical mathematical formulation of the process of permanent regression of tumor, whether spontaneous regression of tumor or therapy-induced regression of the tumor. We now elaborate the clinically-pertinent implications of the research.

4.1. Normal tissue protection

An important aspect of the methodology developed is survival and safeguarding of normal tissue, while at the same time the tumor lesion is being eliminated. Taking care of these two contradictory objectives, our procedure performs the following two contrasting functions:

(i) Minimization of toxicity to the normal tissue due to the antitumor entities: This is done by developing a toxicity cost parameter which is kept minimal using standard Lagrangian method.

(ii) Keeping the concentration of antitumor entities within tolerated ranges: This is done by using physiological limits to the level of DNA damage, cytotoxic T-cells, IL-2, circulating lymphocytes and NK cells.

A major handicap in oncology is that often treatment (chemotherapy and radiotherapy) is started vigorously [50,51], but soon the intervention has to be stopped or downscaled due to the toxicity to normal tissue. Thus, in the latter stage, the tumor proliferates and spreads out through vascular metastasis. In the clinical scenario, an important aspect is that the therapeutic agents may cause considerable damage to normal tissue, such as tissue inflammation and infection, since the normal immunological balance and homeostasis has been impaired due to the drug-induced lysis of the circulating lymphocytes and natural killer cells whereby these cell populations fall below normal protective range. This hazardous condition does not occur in our formulation, since the antitumor entities (or therapeutic agents) and their toxicity functions are always kept within biological bounds, such that the immunological cells (circulating leucocytes and NK cell levels) are always maintained within normal limits, thus protecting against infection and inflammation.

4.2. Robustness of cancer stem cell abolition with negative bias

As is well-known, a critical factor responsible for the failure of tumor containment is the presence of a small side-population of cancer stem cells, which are distinct from the usual cancer cells. Conventional antitumor intervention may act well on the usual cancer cells (the majority part of tumor tissue), the tumor may shrink and become clinically undetectable. However, the small population of cancer stem cells are far more resistant to antitumor drugs since they have drug ejecting efflux-channels, so that these cells survive the drug effect and proliferate continuously, and the tumor soon recurs and disseminates [52]. For instance, the sensitivity of these cancer stem cells to antitumor drugs are only 8–23% of the sensitivity of usual cancer cells to the drug [44].

On the other hand, our negative biasing procedure can successfully eliminate cancer stem cell based tumors, though the time taken is longer than eliminating usual cancer cells. This indicates that more DNA damage induction (i.e., DNA-damaging drug agent) would be needed for lysing the cancer stem cells which are more chemotherapy resistant. However, it may be noted, that there are no normal tissue toxicity issues in our cancer stem cell elimination process, as the physiological bounds are always being maintained. Furthermore, our procedure is robust enough (Figure 9), that is all the malignant stem cells are eliminated even if there is appreciable patient-specific variation in the tumor cell population.

4.3. Double pulsed lymphocyte activation for final tumor eradication

A critical element enabling complete tumor regression is the bimodal activation of antitumor lymphocytes. The requirement of such bimodal activation, one peak each in the initial and in the later phases of the regression process, is corroborated by the experimental studies presented here. In conventional multimodal therapy (Figure 6) where often temporary but not permanent regression occurs, here the T-cell immunotherapy is administered usually at a week's time (day 7–8), and the second peak in T-cell population is absent. We can construe that the second T-cell peak is essential to completely eradicate the residual malignant cells in the late stage of the regression process. Just before the occurrence of the second peak, the tumor cell population is below 5% of the initial tumor population (Figure 7(a)), i.e., the vast majority of the tumor cells has already been eliminated by that time,

nevertheless a second T-cell peak is needed to eliminate the residual tumor cells to prevent relapse. As we have shown, the second peak can be therapeutically induced by suitable dosing of the tumor infiltrating lymphocyte injection from the first day itself (Figure 13(a)), instead of having the week-long delay that customary therapy prescribes. The lack of the second T-cell dosage peak might be a factor why in the well-known clinical trial of the T-cell therapy [53], one observes that the majority of patients (54%) showed no response, while the others showed only a partial response with tumor somewhat shrinking yet remaining extant, a portent of future relapse.

Our cytotoxic T-cells (CTL) immuno-modulation used is of tactical utility, as these cells can exhibit [54] a range of unique behaviors, that chemotherapeutic drugs cannot, such as:

(a) the T-cells can migrate to the primary and secondary growths of the tumor, even in hidden tissue depths,

(b) CTLs can continue to automatically multiply in response to immunogenic proteins of malignant cells, until all those tumor cells become extinct,

(c) T-cells enable immune memory to be stored, allowing further elimination of the tumor, if there is recurrence.

Though our proposal of doublet pulse therapy has not been earlier used in oncology, a doublet pulse approach to cytotoxic therapy has been satisfactorily used in other cell proliferation disorders, as Wegener's granulomatosis [55]. Hence, our proposed double pulse lymphocyte activation procedure may hold appreciable potentiality in the clinical oncology scenario.

4.4. Therapeutic implications of the natural process of spontaneous regression of tumor

Utilizing a systems analysis methodology, our investigation endeavors to elucidate a general unitary basis of tumor regression, which can be applied to both processes: (a) endogenous or spontaneous regression (b) exogenous or therapy-induced regression. Our investigation has formulated that the basic dynamics of both regression processes are comparable and equivalent, and consists of three aspects: (i) DNA interference in malignant cell, (ii) cytokine-based activation of tumor tissue environment (IL-2), and (iii) actuation of antitumor white blood cells (lymphocytes). The paradoxical phenomenon of spontaneous tumor regression has intrigued physicians since the time of St. Peregrines, the patron saint of cancer, these inquirers pondered how the process could be therapeutically replicated on patients, though now the process is known to be much ubiquitous, as the Wisconsin [5] and Scandinavian [4] cancer population registries show.

To analyze the spontaneous cancer regression phenomenon more precisely, we have quantified the regression behaviour in terms of numerically-based DNA interference sites across the tissue (section 2.1 of Supplement). This same DNA interference formulation was shown to apply to drug-induced tumor regression, delineating the unitariness of the two processes. To paraphrase, our investigation of the spontaneous tumor regression process can help design newer modalities of therapeutic regression or treatment. Actually, our approach using three antitumor agents does notably satisfy the requirements needed for mimicking the occurrence of spontaneous tumor regression, as analyzed from the immunoediting perspective. From this immunoediting analysis, the requirements for spontaneous regression are (i) lymphocyte activation (ii) cytokine/interleukin-based activation of antitumor cells (ii) tumor DNA interference using microbial metabolites [56].

4.5. Practical implementation: Enforcement of tumor extinction–computational feedback approach

Our model applied for both endogenous and exogenous tumor regression, the latter implying tumor regression under therapy. Hence our formulation has incisive implications for clinical treatment. A seminal aspect of our formulation is the incorporation of feedback approach (Figure 4), whereby the antitumor entities (DNA damaging entity, interleukin-2, and lymphocytes) are primally and accurately varied with time, such that the tumor cell population undergoes extinction in the specific time duration (around 40–60 days), by following an optimum natural exponentially decreasing trajectory (with negative bias, Figure 1(b)). In other words, this declining curve furnishes the guidance for a trajectory which needs to be followed by the tumor cell population to reach a population of zero in the definitive time period. During the simulation process, after suitable time interval (time-step), one updates the tumor cell population which has declined a bit in the earlier time interval due to the action of the antitumor entities (Section 2.5 and Figure 5). This updated tumor cell population is used (at the next time-step) to determine the new values of antitumor entities, which are implemented iteratively in the simulation loop, and the tumor cell population declines a further bit, so that across successive time intervals, the tumor cell population follows the exponentially decreasing curve to extinction.

As time progresses, and if at any point, there is any incongruence of the actual tumor cell population from the mathematical tumor cell population of the exponential curve, the feedback control system (Figure 5) acts by altering the values of the antitumor entities, so that the error is corrected, and the trajectory of the tumor cell population is also corrected, thereby following the exponential curve. The feedback control approach is in marked contrast to the customary approach in clinical oncology, where the antitumor entities are given in fixed-dose planned out beforehand, and the dosages do not adapt to the variable patient response, and neither to the varying tumor load day-to-day. There were earlier attempts to use feedback control system for antitumor therapy [57] but, as far as we know, they have not been on the lines proposed here, namely trajectory guidance control that enforces the tumor system to persistently reach the target (zero malignant cell population), with inbuilt ability for error correction and adaptation.

4.6. Clinical translation: Towards complete tumor elimination by negative biasing

We can now clarify the modus operandi for clinical applications. We may formulate the generalization of the tissue-induced process of endogenous tumor elimination, so as to develop the therapy-induced process of exogenous tumor regression. For permanently eliminating the tumor, Eqs (9), (11) and (12) respectively provides the required time-varying profile of the intensities of the three entities in the tissue: (i) DNA damage, $D(t)^{\ddagger}$, (ii) cytotoxic lymphocyte population $A(t)^{\ddagger}$, and (iii) cytokine interleukin-2 concentration, $C(t)^{\ddagger}$. In endogenous tumor regression, these levels are generated intrinsically by the host tissue, such as by cellular metabolism and gene activation/deactivation as seen in our analysis of melanoma regression (Figure 12). Likewise, for clinical applicability on patients, we need to induce the exogenous tumor elimination by externally administering therapeutic agents that would produce the requisite temporally-altering levels of the aforesaid entities (i)–(iii), namely the three agents would be a chemotherapeutic agent (e.g., dacarbazine, or cyclophosphamide etc.), cytotoxic T-cells, and interleukin-2 preparation (Figure 2). Each of these agents can be given by time-varying continuous intravenous infusion by an injected fluctuating dose-rate function, $v_{\mathrm{D}}(t)^{\ddagger}$, $v_{\mathrm{A}}(t)^{\ddagger}$ and $v_{\mathrm{C}}(t)^{\ddagger}$ (Section 2.5), which can be readily calculated from the required levels of the three entities

in the tissue $D(t)^{\ddagger}$, $A(t)^{\ddagger}$ and $C(t)^{\ddagger}$ (Figure 5 and Section 2.5). Thus, if those temporal dose-rate patterns of the three therapeutic agents are injected, then the levels of those agents in the tissue would be $D(t)^{\ddagger}$, $A(t)^{\ddagger}$ and $C(t)^{\ddagger}$, whereby the tumor cell population would follow the trajectory in Figure 15, becoming extinct at time t_p days, with no tumor recurrence nor toxicity to the patient.

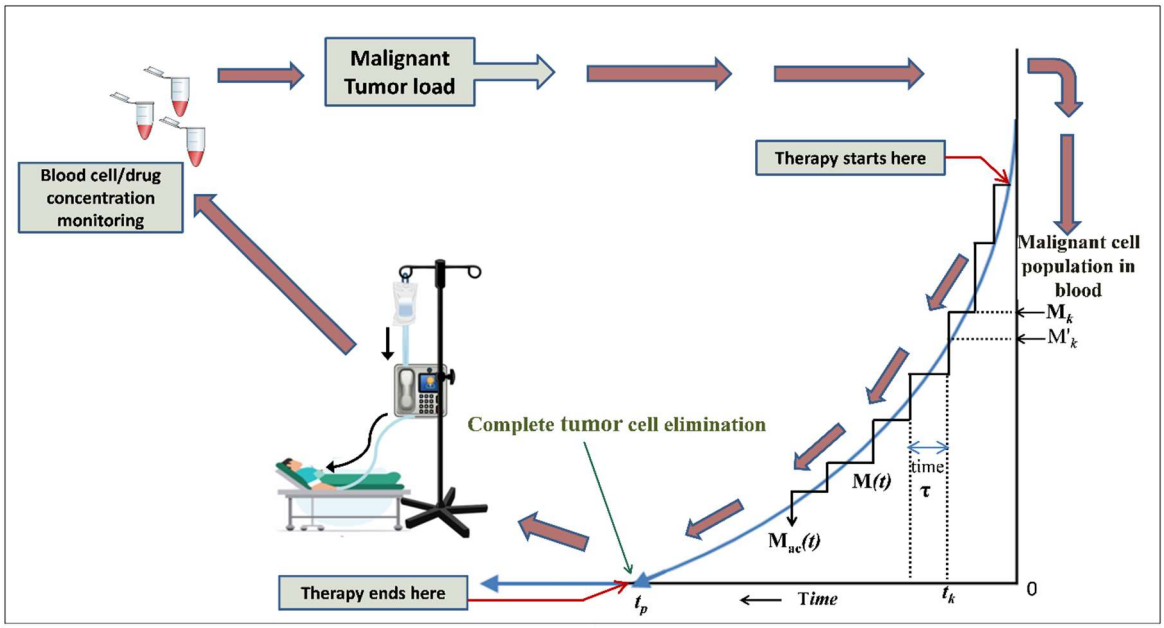

Figure 15. Clinical implementation of the feedback-based tumor elimination procedure, using cytologically-based tumor burden monitoring procedure (e.g., liquid biopsy in blood, or Spect imaging) at weekly time intervals.

5. Conclusions

In retrospect, our approach, validated by experimental findings, shows that a robust quantitative systems biology formulation can be developed to obtain incisive mechanistic insights into the process of complete permanent tumor regression, which often occurs naturally in the form of endogenous spontaneous regression as noted in cancer registries of general populations. Alternatively, the tumor regression process can be replicated therapeutically by antitumor agents, as chemotherapy and immunotherapy. The salient feature of our formulation is that the regression is enabled by very specific but universal characteristics of the antitumor entities, namely single peak level of DNA damaging factor, double pulse level of white blood cell activation (T-lymphocyte), and uniform activation level of the immunomodulator cytokine (IL-2). Indeed, the second pulse feature of lymphocyte activation is an unexpected finding and accounts for the complete extinction of all the residual tumor cells which is in the order of 1% of the initial tumor load. The absence of this second pulse of lymphocytes in customary multimodal therapies may be a factor that prevents these therapies to induce lasting tumor eradication, and one often observes tumor relapse in these cases. Our proposed formulation does not have high-intensity levels of any of the therapeutic agents for a prolonged time, their levels can become much less at intervening times, and there is no appreciable drug-induced toxicity as the immune system (circulating lymphocytes and natural killer cells) are

kept always protected. Thus, it can be suggested that combinational multi-pulsed multimodal therapy, using systems biology based analysis, can offer a principled approach to permanent tumor elimination, with germane implications for the clinical oncology scenario.

Acknowledgments

Bindu Kumari is thankful for the student opportunity furnished by Indian Institute of Technology–Banaras Hindu University, Varanasi. We are thankful for the facilitation extended by iHub NTIHAC Foundation, sponsored by Department of Science and Technology, Ministry of Science and Technology, Govt. of India. For providing research facilitation, Prasun K. Roy is grateful to Shiv Nadar University, his mailing address being Dept. of Life Sciences, R-206, Shiv Nadar University, Dadri, 201316, India.

Conflict of interest

The authors declare that they have no conflict of interest.

References

1. L. T. H. Phi, I. N. Sari, Y. G. Yang, S. H. Lee, N. Jun, K. S. Kim, et al., Cancer Stem Cells (CSCs) in Drug Resistance and their Therapeutic Implications in Cancer Treatment, *Stem Cells Int.,* **2018** (2018), 16. https://doi.org/10.1155/2018/5416923
2. C. J. Wheeler, A. Das, G. Liu, J. S. Yu, K. L. Black, Clinical responsiveness of glioblastoma multiforme to chemotherapy after vaccination, *Clin. Cancer Res*., **10** (2004), 5316–5326. https://doi.org/10.1158/1078-0432.CCR-04-0497
3. R. A. Fenstermaker, M. J. Ciesielski, Immunotherapeutic strategies for malignant glioma, *Cancer Cont.,* **11** (2004), 181–191. https://doi.org/10.1177/107327480401100306
4. P. H. Zahl, P. C. Gøtzsche, J. Mæhlen, Natural history of breast cancers detected in the Swedish mammography screening programme: a cohort study, *Lancet Oncol*., **12** (2011), 1118–1124, https://doi.org/10.1016/S1470-2045(11)70250-9
5. D. G. Fryback, N. K. Stout, M. A. Rosenberg, A. Trentham-Dietz, V. Kuruchittham, P. L. Remington, The Wisconsin breast cancer epidemiology simulation model, *J. Natl. Cancer Inst. Monogr*., **2006** (2006), 37–47, https://doi.org/10.1093/jncimonographs/lgj007
6. T. C. Everson, Spontaneous regression of cancer, *Prog. Clin. Cancer*, **3** (1967), 79–95.
7. "Spontaneous regression of cancer" or "Spontaneous remission of cancer", PubMed, (2022). Available from: https://pubmed.ncbi.nlm.nih.gov/?term=sponteneous+regression+of+cancer+or+sponteneous+remission+of+cancer.
8. H. E. Kaiser, Biological viewpoints of neoplastic regression, *In Vivo,* **8** (1994),155–165.
9. M. C. Perry, D. C. Doll, C. E. Freter, *The Chemotherapy Sourcebook*, Lippincott Williams & Wilkins, Philadelphia, 2012.
10. D. D. Majumder, P. K. Roy, Cancer self-remission and tumour instability–a cybernetic analysis Towards a fresh paradigm for cancer treatment, *Kybernetes,* **29** (2000), 896–927. https://doi.org/10.1108/03684920010342035

11. M. Eisen, *Mathematical Models in Cell Biology and Cancer Chemotherapy, Lecture Notes in Biomathematics*, Springer Berlin, Heidelberg. https://doi.org/10.1007/978-3-642-93126-0
12. A. J. Coldman, J. H. Goldie, A stochastic model for the origin and treatment of tumors containing drug-resistant cells, *Bull. Math. Biol*., **48** (1986), 279–292. https://doi.org/10.1007/BF02459682
13. H. E. Skipper, On mathematical modeling of critical variables in cancer treatment, *Bull. Math. Biol.,* **48** (1986), 253–278. https://doi.org/10.1007/BF02459681
14. N. Bellomo, L. Preziosi, Modelling and mathematical problems related to tumor evolution and its interaction with the immune system, *Math. Comput. Model.*, **32** (2000), 413–452, https://doi.org/10.1016/S0895-7177(00)00143-6
15. C. M. Sakode, R. Padhi, S. Kapoor, V. P. S. Rallabandi, P. K. Roy, Multimodal therapy for complete regression of malignant melanoma using constrained nonlinear optimal dynamic inversion, *Biomed. Signal Process. Control*, **13** (2014), 198–211, https://doi.org/10.1016/j.bspc.2014.04.010
16. I. Osińska, K. Popko, U. Demkow, Perforin: an important player in immune response, *Cent. Eur. J. Immunol.,* **39** (2014), 109–115. https://doi.org/10.5114/ceji.2014.42135
17. M. Bots, J. P. Medema, Granzymes at a glance, *J. Cell. Sci.,* **119** (2006), 5011–5014. https://doi.org/10.1242/jcs.03239
18. H. F. Lodish, A. Berk, C. A. Kaiser, C. Kaiser, M. Krieger, *Molecular Cell Biology*, 4th edition, Macmillan, New York, 2000.
19. A. Bruce, B. Dennis, L. Julian, *Molecular Biology of the Cell (Second Edition)*, Garland Science, New York, (2006).
20. J. S. Orange, Formation and function of the lytic NK-cell immunological synapse, *Nat. Rev. Immunol.*, **8** (2008), 713–725. https://doi.org/10.1038/nri2381
21. M. R. Jenkins, G. M. Griffiths, The synapse and cytolytic machinery of cytotoxic T cells, *Curr. Opin. Immunol.,* **22** (2010), 308–313. https://doi.org/10.1016/j.coi.2010.02.008
22. Spontaneous cancer regression of melanoma, PubMed, (2022). Available from: https://pubmed.ncbi.nlm.nih.gov/?term=spontaneous+cancer+regression+of+melanoma.
23. K. Blessing, K. M. McLaren, Histological regression in primary cutaneous melanoma: recognition, prevalence and significance, *Histopathology,* **20** (1992), 315–322. https://doi.org/10.1111/j.1365-2559.1992.tb00988.x
24. S. Ribero, M. R. Gualano, S. Osella-Abate, Association of histologic regression in primary melanoma with sentinel lymph node status: A systematic review and meta-analysis, *JAMA Dermatol.*, **151** (2015), 1301–1307. https://doi.org/10.1001/jamadermatol.2015.2235
25. Editorial, Melanoma research gathers momentum, *Lancet*, **385** (2015), 2323.
26. I. G. Vladimirova, *Thermodynamics of Biological Processes*, Boston: De Gruyter, Berlin, 1978. https://doi.org/10.1515/9783110860511-027
27. T. Z. Biktimirov, A. A. Butov, Y. G. Savinov, Optimal control of the moment of spontaneous tumor regression, *Automat. Remote Cont.,* **66** (2005), 658–663. https://doi.org/10.1007/s10513-005-0108-z
28. N. Kondo, A. Takahashi, K. Ono, DNA damage induced by alkylating agents and repair pathways, *J. Nucleic Acids,* **2010** (2010). https://doi.org/10.4061/2010/543531
29. E. C. Friedberg, L. D. McDaniel, R. A. Schultz, The role of endogenous and exogenous DNA damage and mutagenesis, *Curr. Opin Genet. Dev.,* **14** (2004), 5–10. https://doi.org/10.1016/j.gde.2003.11.001

30. G. P. Dunn, A. T. Bruce, H. Ikeda, L. J. Old, R. D. Schreiber, Cancer immunoediting: from immunosurveillance to tumor escape, *Nat. Immunol.,* **3** (2002), 991–998. https://doi.org/10.1038/ni1102-991
31. G. P. Dunn, L. J. Old, R. D. Schreiber, The immunobiology of cancer immunosurveillance and immunoediting, *Immunity,* **21** (2004), 137–148. https://doi.org/10.1016/j.immuni.2004.07.017
32. M. Ewend, R. Thompson, R. Anderson, A. K. Sills, K. Staveley-O'Carroll, B. M. Tyler, et al., Intracranial paracrine interleukin-2 therapy stimulates prolonged antitumor immunity that extends outside the central nervous system, *J. Immunother.,* **2** (2000), 435–448. https://doi.org/10.1097/00002371-200007000-00007
33 L. G. de Pillis, W. Gu, A. E. Radunskaya, Mixed immunotherapy and chemotherapy of tumors: modeling, applications and biological interpretations, *J. Theor. Biol.,* **238** (2006), 841–862, https://doi.org/10.1016/j.jtbi.2005.06.037
34. V. A. Kuznetsov, I. L. Makalkin, M. A. Taylor, A. S. Perelson, Nonlinear dynamics of immunogenic tumors: Parameter estimation and global bifurcation analysis, *Bull. Math. Biol.,* **56** (1994), 295–321. https://doi.org/10.1007/BF02460644
35. D. Kirschner, J. C. Panetta, Modeling immunotherapy of the tumor-immune interaction. *J. Math. Biol.,* **37** (1998), 235–252, https://doi.org/10.1007/s002850050127
36. L. G. de Pillis, A. E. Radunskaya, C. L. Wiseman, A validated mathematical model of cell-mediated immune response to tumor growth, *Cancer Res.,* **65** (2005), 7950–7958, https://doi.org/10.1158/0008-5472.CAN-05-0564
37. P. K. Roy, R. Kozma, D. D. Majumder, From neurocomputation to immunocomputation-a model and algorithm for fluctuation-induced instability and phase transition in biological systems, *IEEE Trans. Evol. Comput.*, **6** (2002), 292–305, https://doi.org/10.1109/TEVC.2002.1011542
38. S. Singh, R. Padhi, Automatic path planning and control design for autonomous landing of UAVs using dynamic inversion, *Am. Control Conf.*, **2009** (2009), 2409–2414. https://doi.org/10.1109/ACC.2009.5160444
39. H. Khalil, Nonlinear Systems, 2th edition, in Prentice-Hall, New Jersey, 1996.
40. S. Nanda, H. Moore, S. Lenhart, Optimal control of treatment in a mathematical model of chronic myelogenous leukemia, *Math. Biosci.,* **210** (2007), 143–156, https://doi.org/10.1016/j.mbs.2007.05.003
41. F. Rambow, G. Piton, S. Bouet, J. J. Leplat, S. Baulande, A. Marrau, et al., Gene expression signature for spontaneous cancer regression in melanoma pigs, *Neoplasia,* **10** (2008), 714–726, https://doi.org/10.1593/neo.08344
42. Analyze your own microarray data in R/Bioconductor-BITS wiki., 2022. Available from: https://wiki.bits.vib.be/index.php/Analyze_your_own_microarray_data_in_R/Bioconductor.
43. D. M. Ugo, Does the cell number 10(9) still really fit one gram of tumor tissue?, *Cell Cycle,* **8** (2009), 505–506. https://doi.org/10.4161/cc.8.3.7608
44. J. Foo, F. Michor, Evolution of acquired resistance to anti-cancer therapy, *J. Theor. Biol.*, **355** (2014), 10–20, https://doi.org/10.1016/j.jtbi.2014.02.025
45. A. I. Zotin, *Thermodynamic Bases of Biological Processes: Physiological Reactions and Adaptations*, Walter de Gruyter, Berlin, (1990). https://doi.org/10.1515/9783110849974
46. K. A. Smith, Interleukin-2: inception, impact, and implications, *Science,* **240** (1988), 1169–1176, https://doi.org/10.1126/science.3131876
47. S. Ratner, *Mechanisms of Lymphocyte Extravasation*, 1st edition, S. Karger, Basel, 1992.

48. I. Rousalova, E. Krepela, Granzyme B-induced apoptosis in cancer cells and its regulation. *Int. J. Oncol.,* **37** (2010), 1361–1378, https://doi.org/10.3892/ijo_00000788
49. A. Khar., Mechanisms involved in natural killer cell mediated target cell death leading to spontaneous tumour regression, *J. Biosci.,* **22** (1997), 23–31, https://doi.org/10.1007/BF02703615
50. Q. Gao, G. Zhou, S. J. Lin, R. Paus, Z. C. Yue, How chemotherapy and radiotherapy damage the tissue: Comparative biology lessons from feather and hair models, *Exp. Dermatol,* **28** (2019), 413–418. https://doi.org/10.1111/exd.13846
51. C. Yarana, D. K.St. Clair, Chemotherapy-induced tissue injury: An insight into the role of extracellular vesicles-mediated oxidative stress responses, *Antioxidants (Basel),* **6** (2017), 75. https://doi.org/10.3390/antiox6040075
52. A. Z. Ayob, T. S. Ramasamy, Cancer stem cells as key drivers of tumour progression, *J. Biomed. Sci.,* **25** (2018), 20. https://doi.org/10.1186/s12929-018-0426-4
53. M. E. Dudley, J. R. Wunderlich, P. F. Robbins, J. C. Yang, P. Hwu, D. J. Schwartzentruber, et al., Cancer regression and autoimmunity in patients after clonal repopulation with antitumor lymphocytes, *Science,* **298** (2002), 850–854, https://doi.org/10.1126/science.1076514
54. M. L. Disis, H. Bernhard, E. M. Jaffee, Use of tumour-responsive T cells as cancer treatment, *Lancet,* **373** (2009), 673–683. https://doi.org/10.1016/S0140-6736(09)60404-9
55. A. Radbruch, A. Thiel, Cell therapy for autoimmune diseases: does it have a future, *Ann. Rheum. Dis.,* **63** (2004), 96–101. http://dx.doi.org/10.1136/ard.2004.028340
56. N. Sengupta, T. S. MacFie, T. T. MacDonald, D. Pennington, A. R. Silver, Cancer immunoediting and "spontaneous" tumor regression, *Pathol. Res. Pract*., **206** (2010), 1–8. https://doi.org/10.1016/j.prp.2009.10.001
57. R. Martin, K. L. Teo, Optimal control of drug administration in cancer chemotherapy, *World Sci.*, **1993** (1993), 204. https://doi.org/10.1142/2048

AIMS Press